

# DEVELOPMENT OF Ni-P-ZnO NANOCOMPOSITE COATINGS

A DISSERTATION

*Submitted in partial fulfillment of the  
requirements for the award of the degree*

of

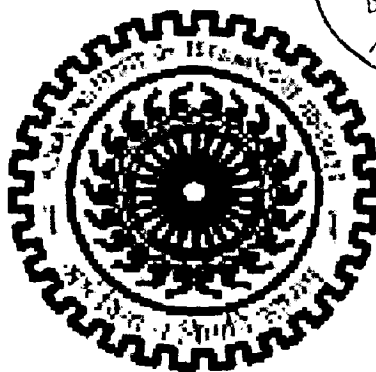
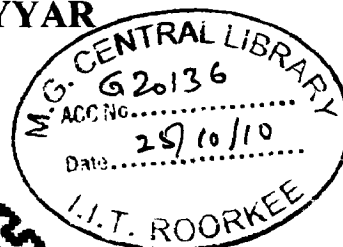
MASTER OF TECHNOLOGY

in

NANOTECHNOLOGY

By

RAJ KARAN NAYYAR



CENTRE OF NANOTECHNOLOGY  
INDIAN INSTITUTE OF TECHNOLOGY ROORKEE  
ROORKEE – 247 667 (INDIA)  
JUNE, 2010

## CANDIDATE'S DECLARATION


---

I hereby declare that the work presented as the dissertation thesis entitled "Development of Ni-P-ZnO nanocomposite coatings" in partial fulfillment of requirements for the award of the Master of Technology in Nanotechnology in Centre of Nanotechnology, Indian Institute of Technology Roorkee, India, is an authentic record of my own work carried under the guidance of Dr. VIJAYA AGARWALA, Joint faculty, Centre of Nanotechnology and MMED and Dr. R. C. AGARWALA, Professor, MMED, Indian Institute of Technology Roorkee, India.

The matter submitted in this seminar has not been submitted by me for the award of any other degree.

Date: 30/6/10

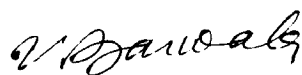
Place: Roorkee

  
(Raj Karan Nayyar)  
(08551008)

## CERTIFICATE

---

This is to certify that the above statement made by the candidate is correct to the best of our knowledge and belief.



(Dr. VIJAYA AGARWALA)

Joint Faculty

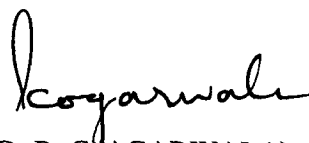
Centre of Nanotechnology

and

MMED

Indian Institute Technology

Roorkee, Uttarakhand, India



(Dr. R. C. AGARWALA)

Professor

MMED

Indian Institute Technology

Roorkee, Uttarakhand, India

## ACKNOWLEDGEMENT

---

It gives me great pleasure to take this opportunity to thank and express my deep sense of gratitude to Dr. Vijaya Agarwala, Joint Faculty, Centre of Nanotechnology and Department of MME, Dr. R. C. Agarwala, professor, Department of MME, and Dr. Naveen Kumar Navani, Department of Biotechnology, Indian Institute of Technology, Roorkee for their invaluable guidance throughout the period of this dissertation work. Further I am thankful to them for all the inspiration and motivation they inculcated in me.

I am obliged to Dr. Anil Kumar, Professor and Head, Centre of Nanotechnology and Dr. P. K. Ghosh, Head Department of MME for creating the right infrastructure and facilities conducive to my dissertation work. I express my sincere thanks to them for their kind help and moral support throughout this dissertation work.

I am also very thankful to Head of the Institute Instrumentation Centre for providing necessary facilities for this work.

Thanks are due to the entire staff of the department for their help and assistance.

My special sincere heartfelt gratitude to my seniors especially Mr. Sachin Tyagi and Mr. Devesh Devdutt Mishra, Research scholars, Department of MME, Ms. Supriya, Research scholar, Department of Biotechnology, Indian Institute of Technology.

I am also grateful to my friends especially Jitendra Pal, Ankur Anand, Gouri Trehan, Rajesh Kumar U. who were actively involved in providing me vital support and encouragement whenever I needed.

I would like to express my gratitude to my parents; their blessings, motivation and inspiration have always provided me a high mental support and contributed in all possible way, in completion of this project work.

## ABSTRACT

---

Zinc oxide nanoparticles can be synthesized by physical methods or chemical methods or combinations of both, the chemical method are useful for getting very small size nanoparticles. The nanoparticles are known for a wide variety of applications like UV absorbing properties, antibacterial characteristics and so on.

Electroless(EL) co-deposition of particles, represent a method to obtain metal matrix composite materials as thin foils (coatings) at low temperature (90<sup>0</sup>C). The particles can be synthesized in the bath or added externally to the bath. During the redox reaction between Ni ions and sodium hypophosphite, the particles are physically entrapped in a growing Ni-P layer on the substrate surface.

In the present study, synthesis and characterization of a new electroless Ni-P based nanocomposite coatings on mild steel substrate have been carried out. Nanoparticles of Zinc oxide were synthesized through physical method by Ball milling and chemical method by sol-gel technique and co-deposited. The synthesized nanocomposite coatings were characterized by X-Ray Diffraction, FE-SEM, EDAX and AFM analysis.

# CONTENTS

---

	<b>Page No.</b>
<b>CANDIDATE'S DECLARATION</b>	<b>i</b>
<b>ACKNOWLEDGEMENT</b>	<b>ii</b>
<b>ABSTRACT</b>	<b>iii</b>
<b>CONTENTS</b>	<b>iv-v</b>
<b>LIST OF FIGURES</b>	<b>vi-vii</b>
<b>LIST OF TABLES</b>	<b>viii</b>
<b>Chapter 1 INTRODUCTION</b>	<b>1-2</b>
<b>Chapter 2 REVIEW OF LITERATURE</b>	<b>3-21</b>
2.1 Synthesis of Zinc oxide Nanoparticles	3-7
2.1.1 Sol-gel method of synthesis	4
2.1.2 Mechano-chemical synthesis	6
2.2 Electroless coating technology	7-14
2.2.1 History of electroless deposition	7
2.2.2 Bath composition and characteristics	9
2.2.3 Factors affecting the coating process	13
2.3 Electroless composite coating	14-16
2.3.1 Mechanism of particle incorporation	15
2.3.2 Factors influencing particle incorporation	16
2.4 Applications of zinc oxide	16-18
2.4.1 Present applications	16
2.4.2 Future applications	17
2.5 Applications of Electroless nickel coating	18
<b>Chapter 3 FORMULATION OF PROBLEM</b>	<b>22-23</b>

---

<b>Chapter 4 EXPERIMENTAL WORK</b>	<b>24-38</b>
4.1 Materials and instruments used	24-25
4.1.1 Chemical salts and reagents used	24
4.1.2 Instruments and equipments used	24
4.2 Synthesis of zinc oxide nanoparticles by mechano-chemical synthesis	26
4.3 Synthesis of Zinc oxide by sol-gel method	27
4.4 Synthesis of Ni-P-ZnO nanocomposite coating	28-30
4.4.1 Substrate preparation and pre-treatment	28
4.4.2 Steps for surface preparation	28
4.4.3 Surface pre-treatment	28
4.4.4 Bath Composition and Operating Conditions	28
4.4.5 Process details	29
4.4.6 Procedure	30
4.4.7 Precautions	30
4.5 Characterisation techniques	31-36
4.5.1 X-Ray Diffraction analysis	31
4.5.2 FESEM analysis	32
4.5.3 EDAX analysis	36
4.5.4 AFM analysis	37
<b>Chapter 5 RESULTS AND DISCUSSION</b>	<b>39-51</b>
5.1 Characterisation of zinc oxide nanoparticles	39-44
5.1.1 Zinc oxide prepared through physical method	39
5.1.1.1 X-Ray Diffraction results	39
5.1.1.2 FESEM results	41

5.1.2 Zinc oxide prepared through chemical method	43
5.1.2.1 X-Ray Diffraction results	43
5.1.2.2 FESEM results	44
5.1.2.3 EDAX analysis	44
5.2 Characterisation of nanocomposite coating	45-51
5.2.1 X-Ray Diffraction results	45
5.2.2 FESEM results	46
5.2.3 EDAX analysis	48
5.2.4 AFM analysis	49
<b>PRECAUTIONS</b>	<b>52</b>
<b>CONCLUSIONS</b>	<b>53</b>
<b>FUTURE SCOPE</b>	<b>54</b>
<b>REFERENCES</b>	

# LIST OF FIGURES

---

<b>Figure No.</b>	<b>Description</b>	<b>Page No.</b>
Fig. 4.1 (a)	PM 400/2 High Energy planetary Ball Mill	25
Fig. 4.1 (b)	Electric Furnace	25
Fig. 4.1 (c)	Electroless Bath	25
Fig. 4.1 (d)	pH Meter	25
Fig. 4.1 (e)	Elix Milipore for Distilled water	25
Fig. 4.1 (f)	Bruker D-8 Advance	25
Fig. 4.2	Schematic diagram of the experimental set-up used for EL coating bath	29
Fig. 4.3	Emissions in SEM	35
Fig. 5.1	X-Ray Diffraction pattern of Synthesis steps of ZnO	40
Fig. 5.2(a)	FE-SEM image of 25 hours milled sample at 40000x magnification	41
Fig. 5.2(b)	FE-SEM image of 45 hours milled sample at 20000x magnification	42
Fig. 5.2(c)	FE-SEM image of 45 hours milled sample heated at 600 <sup>o</sup> C, after washing with De-ionised water at 100000x magnification	42
Fig. 5.3	X-Ray Diffraction pattern of Zinc oxide prepared through sol-gel method	43
Fig. 5.4	FE-SEM of Zinc oxide prepared through sol-gel route	44

---



Fig.5.5	EDAX pattern of Zinc oxide prepared through sol-gel method	44
Fig.5.6	X-Ray Diffraction pattern of Synthesis steps of Nano-composite coating	45
Fig.5.7(a)	FE-SEM of sample coated with Ni-P	46
Fig.5.7(b)	FE-SEM of sample coated with Ni-P-ZnO	46
Fig.5.7(c)	FE-SEM of sample coated with Ni-P-ZnO	47
Fig.5.7(d)	FE-SEM of sample coated with Ni-P-ZnO followed by heat treatment	47
Fig.5.7(e)	FE-SEM of sample coated with Ni-P-ZnO followed by heat treatment	47
Fig.5.8(a)	EDAX of sample coated with Ni-P	48
Fig.5.8(b)	EDAX of sample coated with Ni-P-ZnO	48
Fig.5.8(c)	EDAX of sample coated with Ni-P-ZnO followed by heat treatment	48
Fig.5.9(a)	AFM Pattern of sample coated with Ni-P showing 3D pattern, surface pattern, roughness	49
Fig.5.9(b)	AFM Pattern of sample coated with Ni-P-ZnO showing 3D pattern, surface pattern, roughness	50
Fig.5.9(c)	AFM Pattern of sample coated with Ni-P-ZnO after heat treatment showing 3D pattern, surface pattern, roughness	51

# LIST OF TABLES

---

<b>Table No.</b>	<b>Description</b>	<b>Page No.</b>
Table 2.1	Different Electroless Alloy Coating Developed and Primarily referred in the Literature	15
Table 4.1	Bath composition and Operating conditions	29
Table 5.1	Elemental composition of Zinc oxide prepared through sol-gel method	44
Table 5.2(a)	Elemental composition of sample coated with Ni-P	48
Table 5.2(b)	Elemental composition of sample coated with Ni-P-ZnO	48
Table 5.2(c)	Elemental composition of sample coated with Ni-P-ZnO followed by heat treatment	48
Table 5.3(a)	AFM measurements of sample coated with Ni-P	49
Table 5.3(b)	AFM measurements of sample coated with Ni-P-ZnO	50
Table 5.3(c)	AFM measurements of sample coated with Ni-P-ZnO followed by heat treatment	51

Nanocomposite coatings are defined to have either the thickness of coatings or the dispersed second phase particles into the matrix, in the nanosize range. Nanocomposite coating is the most promising novel concept developed in the coating technology. There exists an increasing amount of on-going research focused on the selection of the constituent phases of a nanocomposite, and the modification of coating's microstructure, in order to synthesize novel nanocomposite coating systems. On the other hand, most applications have complex requirements for the physical, chemical and mechanical properties of the coating and in most cases a single coating cannot satisfy all these requirements. Thus coating materials with different properties and novel coating concepts can all be engineered into an appropriate coating architecture to meet a specific application.[1]

Electroless nickel-based composite coatings use the conventional EL reduction reaction process with suspension of the particles (externally added) during the coating process. Such electroless composite coatings are becoming more popular for engineering applications. In this process, during the redox reaction between  $\text{Ni}^{2+}$  ions and hypophosphite, the inert particles are physically entrapped in the growing layer of Ni-P coating. Using the preceding coating method, composite layers with tailored characteristics/properties for specific applications can be produced. Further, to improve the properties of the matrix of EL deposits, it is subjected to a suitable heat treatment after coating. Generally, during codepositing the particles in EL, concentration of particles in deposits depend on various factors such as bath chemistry, particle characteristics, and operating conditions. Each combination between a certain type of particles and the Ni-P matrix can lead to a new set of properties of the composite coatings. Electroless coatings are being increasingly used because of their unique physicochemical and mechanical properties. The electroless deposition can provide uniform thickness of the coating, ranging from 2.5 to 500  $\mu\text{m}$ , even on the complex

geometrical components over the entire area, unlike electroplating, which provides uneven thickness of coating at corners and awkwardly located areas. Electroless nickel-based coatings offer effective barrier properties in electronic chips and corrosion resistance, owing to their amorphous nature and pore-free networks.

Nanosized particles have a larger surface area per unit mass and hence higher efficiency than bulk materials. Inorganic materials such as metal and metal oxides have attracted a lot of attention because of their ability to withstand harsh processing conditions. One of these inorganic materials is zinc oxide (ZnO). ZnO belongs to a group of metal oxides that are characterized by the following properties: photo catalytic ability, electrical conductivity, UV absorption; photo oxidizing capacity versus chemical and biological species, antimicrobial, and self-sterilization (2). Moreover, ZnO is generally regarded as a safe material for human beings and animals, and it has been used extensively in the formulation of personal care products (3,4).

In this investigation ZnO nanoparticles were synthesized by physicochemical method and sol-gel method, physical method provides the advantage of production in large quantity economically, chemical method provides the advantage of size control. ZnO nanoparticles synthesized were then codeposited along with Ni-P on mild steel substrate by electroless coating technique.

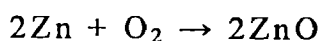
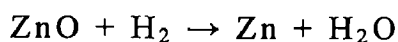
## CHAPTER 2

### LITERATURE REVIEW

---

#### 2.1) Synthesis of Zinc Oxide Nanoparticles:

Bulk ZnO samples are grown by various techniques. A possibility to grow ZnO by gas transport is given by the following reactions:



Sometimes graphite is used for the reduction of Zn instead of H<sub>2</sub>. Pressed or sintered samples of high-purity ZnO powder are reduced to Zn vapour at elevated temperatures by hydrogen (or the addition of graphite) which is transported with a flow of inert gas like N<sub>2</sub>. The zinc vapour is then oxidized in a region of lower temperature under the admission of oxygen or air. Platelets and particularly beautiful hexagonal needles can be grown with diameters up to several mm and length of several. Alternatively, one can start directly with Zn vapour. Some selected references for gas-transport techniques are, e.g. [5,6].

A number of investigations on the synthesis of ZnO nanoparticles have been reported in the literature [7–13]. There have been several reports of solution-phase synthesis of ZnO nanoparticles at low temperature. The synthesis of these particles is mainly based on the alcoholic hydrolysis of zinc precursors [14,15], hydrothermal methods [16] and electrochemical routes [17]. Among these techniques, the hydrolysis route is very attractive because it is relatively easy to perform and allows us to tailor the morphology of the particles by controlling the rate of hydrolysis and condensation reactions [18]. Hossain et al. [18] have obtained nanobelts of ZnO of length 700 nm using refluxing technique. Several workers have used capping agent such as vinyl pyridine (PVP), polyethylene glycol (PEG), etc. to stop particle agglomeration and obtained nanoparticles of size less than 5 nm [19,20]. One hydrothermal method commonly used to synthesize

ZnO for more than 50 years[21,22] is to grow single crystals (generally > 5 cm) by then slow dissolution of ZnO powder held at a higher temperature relative to a ZnO “seed” crystal held at a lower temperature, all within a high temperature (generally > 300 °C) autoclave. Generally, “mineralizers” such as KOH, NaOH, and NH<sub>4</sub>OH are used to increase the solubility of ZnO powder and thus to increase the growth rate of the single crystals. A second hydrothermal method uses a zinc salt such as ZnCl<sub>2</sub>,[23] Zn(NO<sub>3</sub>)<sub>2</sub>,[24] or Zn(CH<sub>3</sub>COO)<sub>2</sub>[25,26] to synthesize ZnO powders with different particle morphologies at lower temperatures (80 °C to 200 °C) for this second method..

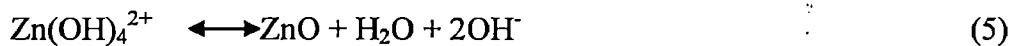
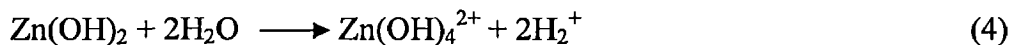
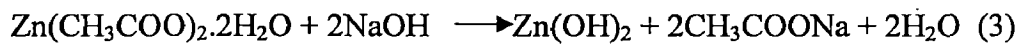
Much research has been focused on the preparation and the properties of ZnO nanocrystals; however, little of it dealt with the pH effect of the sol on the crystallite size of ZnO powder. For instance, Li et al. [27] concluded that the solution conditions have a certain effect on the particle size of ZnO powders under hydrothermal conditions. Zhang et al. [28] found that the pH value can change the quantity of ZnO nuclei and of growth units. Lu and Yeh [29] found that the characteristics of ZnO powder profoundly depend on the pH of the starting solutions. In addition the crystallinity and particle size of ZnO powder increase with a rise in the pH of solution.

#### **2.1.1) Sol-gel method of synthesis[30]:**

In this work ZnO powder was synthesized using sol–gel route. Zinc acetate dihydrate was used as a precursor due to easier control of hydrolysis.

The ZnO sols were prepared by dissolving zinc acetate dihydrate (99.5% (CH<sub>3</sub>COO)<sub>2</sub>Zn·2H<sub>2</sub>O, Merck) in methanol at room temperature. A clear solution of 0.2 M was obtained by ultrasonic magnetic stirrer at 25 °C for 120 min. The sol prepared was found to be stable and transparent with no precipitate or turbidity. ZnO powders were prepared by varying the pH value of sol from 6 to 11. The pH value of the sols was adjusted to the desired value using sodium hydroxide (0.1 N NaOH, Merck) solution. The modified sols were stirred ultrasonically for 60 min at room temperature. The clear solution was filtered through micron filter paper. The resulting transparent filtrate was kept for 48 h to complete the gelation and hydrolysis process. During this period of time, white ZnO precipitates were slowly crystallized and settled down in the bottom of the

flask. The white precipitate was filtered and washed with excess methanol to remove the starting materials and dried at 120 °C for 2 h. The acidic nature of the sol ( $\leq 6$ ) prevents the easy precipitation of ZnO powder at room temperature. The growth of ZnO from zinc acetate dihydrate precursor using sol-gel process generally undergoes four stages, such as solvation, hydrolysis, polymerization and transformation into ZnO. The zinc acetate dihydrate precursor was first solvated in methanol, and then hydrolyzed, regarded as removal of the intercalated acetate ions and results in a colloidal-gel of zinc hydroxide (Eq. (3)). The size and activity of solvent have obvious influence on the reacting progress and product. Methanol has smaller size and a more active -OH and -OCH<sub>3</sub> groups. Methanol can react more easily to form a polymer precursor with a higher polymerization degree, which is required to convert sol into gel [31]. These zinc hydroxide splits into Zn<sup>2+</sup> cation and OH<sup>-</sup> anion according to reactions (Eq.(4)) and followed by polymerization of hydroxyl complex to form “Zn-O-Zn” bridges and finally transformed into ZnO (Eq. (5)) [32]



When the concentration of OH<sup>-</sup>, i.e. pH is low, the growth of ZnO particle does not proceed because of the lack of Zn(OH)<sub>2</sub> formation in the solution. Therefore, in sol-gel technique there is a threshold pH level above which the nanostructure may be formed. In this study, the growth of ZnO nanoparticles in zinc acetate solution was observed from a solution having pH of 7. A solution with a pH of 7 would have insufficient OH<sup>-</sup> concentration to synthesize ZnO which is also clear from XRD pattern. Since pH controls the rate of ZnO formation, it affects the size and their way of combination to get stable state. As the freshly formed nuclei in the solution are unstable, it has a tendency to grow into larger particles. The largest crystallite size was observed when the pH of the solution was 9. Further increase in the concentration of OH<sup>-</sup> from this point, reduced the crystallite size of ZnO. This is presumed to be because of the dissolution of ZnO (back reaction of Eq. (5)). When ZnO reacts with OH<sup>-</sup>, the dissolution of ZnO occurs [33].

The continuous decrease in crystallite size above 9pH level as seen from Fig. 2 is the evidence of the acceleration of ZnO dissolution during competitive ZnO formation. The secondary ZnO (1mm) particles as observed by SEM images consist of primary ZnO nanocrystallites (10 nm). The primary nanocrystallites can combined to form a larger particle (secondary) by the following two routes [34]:

(1) Fusion of one primary crystallite (10 nm) into another.

(2) Aggregation of the primary crystallites (10 nm).

The first mechanism will yield a large particle giving crystallite size of micrometer scale (mm). The second route will result a bigger particle consisting of primary (10 nm) subunits with porosity. In the present work it appears that the aggregation is the dominant mechanism which occurred during the crystallization of gel network leading to macroscopic ZnO particles.

### **2.1.2 Mechanochemical synthesis[35]:**

Milling of precursor powders leads to the formation of a nanoscale composite structure of the starting materials that react during milling or subsequent heat treatment to form a mixture of separated nanocrystals of the desired phase within a soluble salt matrix. The separation of the nanoparticles will occur due to existence of NaCl that prevents the subsequent agglomeration ZnO nanoparticles during calcination. Removal of the salt matrix is usually carried out through simple washing. For example, ultrafine ZnO powder was synthesized by the milling and subsequent heat treatment of a ZnCl<sub>2</sub>, NaCl and Na<sub>2</sub>CO<sub>3</sub> powder mixture. Removal of the NaCl with a simple washing process resulted in separated ZnO particles [36-38].

The starting materials were anhydrous ZnCl<sub>2</sub> granules (Merck,99.5%), Na<sub>2</sub>CO<sub>3</sub> powder (Merck,99%) and NaCl (Merck,99%). All the starting materials were dried in air at 150°C. A stoichiometric mixture of the starting materials was milled corresponding to the following reaction equation:





NaCl was added to the reactants so that the volume ratio of the ZnCO<sub>3</sub>: NaCl in the product phase was 1:10. The NaCl was used as an inert diluent and added to the starting powders. The mixture of starting powders was milled in a ball mill with zirconia balls of 10mm in diameter and 250 rpm. The precursor was calcined at 400°C in air in a porcelain crucible to prepare the ZnO nanoparticles. Since the mechanochemically formed ZnCO<sub>3</sub> nanoparticles were isolated in the NaCl matrix, sintering of the ZnO powder did not occur during heat treatment. Removal of the salt by-product was carried out by washing the powder with de-ionised water. The washed powder was dried in a spray drier.

## **2.2 Electroless Coating Technology:**

Electroless coating is the name given originally by A. Brenner and G. Riddell to a method of coating metallic bodies, with an nano crystalline nickel or cobalt- phosphorus alloy through controlled autocatalytic reduction of cations (Ni<sup>++</sup> or Co<sup>++</sup>) at the surface of said body by means of hypophosphite anions (H<sub>2</sub>PO<sub>2</sub><sup>-</sup>) in aqueous medium, without the use of an external source of electric current.[Kenneth graham a. 1971]. Electroless, EL (without using electricity) is one of the best coating technology in which deposition is purely systematic chemical process, i.e., sensitization, activation, nucleation and growth of nanosized alloy or composite globules first horizontally then vertically during the reduction process onto the catalytic surface of the substrate.[39] Here it is important to state that the deposition rate in the horizontal direction is faster than vertical direction, and this makes the coating pore free.

### **2.2.1 History of Electroless Deposition**

The metallic nickel from aqueous solution in presence of hypophosphite was first noted in the year 1844, as a chemical curiosity by Wurtz, and later, Breteau in 1911 inevitably precipitated the metal in powder form, which was deposited on the surface of reaction vessels as bright coatings.[40,41] A similar work by Roux had led to further development in the year 1946 as proclaimed in the work of Gillespie.[42] After its illustrious rediscovery by Brenner and Riddell in 1946,[41] interest of the scientific community in this field was aroused; this resulted in a large number of investigations on various aspects

of the fascinating novel technique to coat the materials. While pursuing for improved corrosion resistance of the coating, the composite coatings were carried out for electrodeposited nickel-chromium by Odekerken[43] during the year 1966. Also, their efforts credited the first commercial application of EL Ni-SiC coatings on the Wankel (rotary) internal combustion engine.[44] In the year 1981, a commercial composite coating Ni-P-PTFE (polytetrafluoroethylene) was introduced in contrast to the difficulties encountered with diamond and PTFE particles, composites incorporating alumina or silicon carbide have been achieved without serious difficulties.[45] Thus, the ability to co-deposit fine second phase particles (of size range of varying from micron to nano level) within a metal/ alloy matrix has led to a new generation of composite coatings. It is reported that the amorphous EL Ni-P “as-coated”, when heat-treated is found to precipitate nanocrystalline Ni and nickel phosphide phase.[46,47] The variation of magnetic moments and energy with temperature has been studied for various amorphous coatings.[47–49] Auto-catalytically deposited Ni-P amorphous alloys have many industrial applications because of their paramagnetic properties, excellent resistance to wear and corrosion, and high hardness matching with hard electro deposited chromium. Metal/alloy coatings of copper, [50,51] Ag, [52] Ni-P,[46,53–55] and Ni-B,[56,57] have been reported. The bonding mechanism of the EL nano Cu and Ni-P coatings have been evaluated for different substrates like ceramic powder, glass and Al sheet. All the coating have been reported to have good adherence with the substrate.[50,51] The co-deposition efficiency of the second phase particles reinforced in the matrix depends on the size, shape, density, polarity, concentration and method of suspension in the bath has reported in the literature, but different studies have reported different results.[39] Apart from plating by reduction reaction, two other methods have also been reported. These include immersion plating on steel from solutions of nickel chloride and boric acid, and decomposition of nickel carbonyl vapour on steel substrate (Parker 1972; Gaurilow 1979). However, the latter is hazardous and former is poorly adherent and non-protective. The advantage of using the autocatalytic reduction reaction is in maintaining overall uniformity of coating in composition and thickness which is independent of the thickness variations of the substrate (Agarwala 1987). Several binary and ternary alloys have been deposited, these include the investigations of Ni-P (Brenner & Riddell 1946; Graham et

al 1962, 1965; Henry 1984; Harris 1985; Bakonyi et al 1986; Agarwala 1987; Husheng et al 1991; Andre et al 1993; Paunovic et al 1995; Puchi et al 1997; Chitty et al 1997; Bozzini & Boniardi 1997; Bozzini et al 1999; Balaraju & Sheshadri 1999; Apachitei & Duszczuk 2000), Ni-B (Datta et al 1991; Srivastava et al 1992; Di Giampaolo et al 1997; Vasudevan et al 1998), Ni-Cu-P, Ni-Re-P (Gorbunova et al 1966), Ni-W-P (Pearlstein et al 1963; Li et al 1996), Co-P, Co-B (Brenner et al 1950), Fe-Mo-W-B (Wang et al 1997), Ni-Co-P (Kim et al 1995; Wang et al 1997), Fe-Sn-B, Fe-W-B, Fe-Mo-B (Wang et al 1997) and Ni-Sn-Cu-P (Bangwei et al 1999). Different alloys are coated for desired physical and mechanical properties. Nickel turns out to be the single most widely coated element with phosphorous. Apart from nickel, many alloys contain at least one of the elements Co, Cu, Pd, Pt, Au or Ag.

### **2.2.2 Bath composition and characteristics**

Mainly two types of baths have been used for depositing alloys. These include acidic and alkaline baths. Electroless alloy coatings are produced by the controlled chemical reduction of metallic ions onto a catalytic surface, the deposit/coating itself is catalytic to the reduction reaction and the reaction continues as long as the surface remains in contact with the bath solution or the solution gets depleted of solute metallic ions. The coating is uniform throughout the contours of the substrate because no electric current is used. Therefore, all parts of the surface area of substrate which are equally immersed in the bath have equal probability of getting ions deposited. The bath (electrolytic) characteristics have been considered by taking nickel as an example.

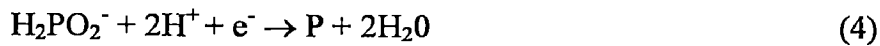
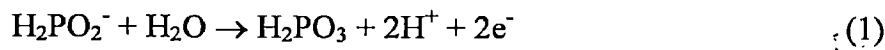
A source of nickel ions, usually nickel sulphate or nickel chloride is used other than this the electroless bath solution comprises of different chemicals each performing an important function (Agarwala 1987) as below.

- A reducing agent to supply electrons for the reduction of nickel
- Energy (heat)
- Completing agents (chelates) to control the free nickel available to the reaction

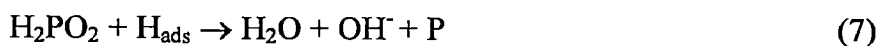
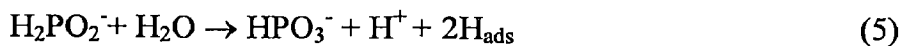
**2.2.2a Reducing agents:** Several reducing agents have been used in electroless coating of alloys. Four types of reducing agent have been used for electroless nickel bath including sodium hypophosphite, amineboranes, sodium borohydride, and hydrazine.

(i) **Sodium hypophosphite baths** – More than 70% electroless nickel is deposited from solutions reduced by sodium hypophosphite. The main advantage of these solutions over those reduced by borohydride or hydrazine includes lower costs, greater ease of process control etc. Several mechanisms have been proposed for the chemical reactions that occur in hypophosphite reduced electroless nickel plating solutions. Most widely accepted mechanisms are illustrated by the following equations (Gutzeit 1959, 1960).

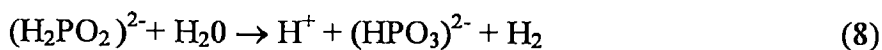
**Electrochemical mechanism**, where catalytic oxidation of the hypophosphite yield electrons at the catalytic surface which in turn reduces nickel and hydrogen ions is illustrated below:



**Atomic hydrogen mechanism**, where atomic hydrogen is released as the result of the catalytic dehydrogenation of hypophosphite molecule adsorbed at the surface is illustrated below.



The adsorbed active hydrogen, (6) then reduces nickel at the surface of the catalyst.



Simultaneously, some of the absorbed hydrogen reduces a small amount of the hypophosphite at the catalytic surface to water, hydroxyl ion and phosphorus, (7). Most of the hypophosphite present is catalytic, which is oxidized to orthophosphite and gaseous hydrogen, (8), causing low efficiency of electroless nickel solutions for alloy coating while the deposition of nickel and phosphorus continues. Usually, 5 kg of sodium hypophosphite is required to reduce 1 kg of nickel, for an average efficiency of 37% (Mallory 1974; Gaurilow 1979). The coefficient of utilization of hypophosphite vary a little with the nature of buffer additive; the highest degree of utilization of the hypophosphite was observed in the solution containing sodium acetate, the lowest is that with sodium citrate. The main characteristic of the process is the change in the composition of the solution. The concentration of nickel salt and hypophosphite is decreased and the concentration of acid is increased during the progress of deposition. This causes the lowering of deposition rate (Mallory 1974).

(ii) **Amineborane baths** – Use of amineboranes in electroless Ni plating solutions have been limited to two compounds: N-dimethylamine borane .DMAB/-.CH<sub>3</sub>/2NHBH<sub>3</sub>, and H diethylamine borane .DEAB/-.C<sub>2</sub>H<sub>5</sub>/2NHBH<sub>3</sub> (Gaurilow 1979; Mallory 1979; Stallman & Speakhardt 1981). DEAB is used primarily in European establishments, whereas DMAB is used generally in USA. DMAB is readily soluble in aqueous solutions while DEAB should be mixed with a short chain aliphatic alcohol such as ethanol, before mixing into plating bath. The amineboranes are effective reducing agents over a wide range of pH but due to evolution of hydrogen, there exists a lower limit of pH up to which the plating process can be carried out (Mallory 1979). Nickel, in the deposit increases as pH of the bath increases. Usually, the amineborane baths have been used in the pH range of 6 to 9. Operating temperatures for these baths range from 50–80<sup>0</sup>C, however, they can be used at temperature as low as 30<sup>0</sup>C. Accordingly, amineborane baths are very useful for plating non-catalytic surfaces such as plastics, non-metals, which are their primary applications. The rate of depositions varies with pH and temperature, but is usually 7 to 12µm/h.

(iii) **Sodium borohydride baths** – The borohydride ion is the most powerful reducing agent available for electroless nickel plating. Any water-soluble borohydride can be used;

however, for optimum results sodium borohydride is preferred (Mallory 1974). In acid or neutral solutions, hydrolysis of borohydride ions is very rapid. In the presence of nickel ions nickel boride may form spontaneously. If the pH of the solutions is maintained between 12 and 14 the formation of nickel boride is suppressed and the reaction product is principally elemental nickel. One mol. of sodium borohydride can reduce approximately one mol. of nickel, it can be deduced that the reduction of 1 kg of nickel requires 0.6 kg of sodium borohydride while 5 kg of hypophosphite is required. Deposits from borohydride reduced electroless nickel contain 3 to 8 wt% boron. To prevent precipitation of nickel hydroxide, complexing agents such as ethylenediamine, that are effective between 12 to 14 pH must be used. The presence of such complexing agents, however reduces the reaction rate thereby lowering the rate of deposition. At operating temperatures of 90°C the rate of deposition lies somewhere 25 to 30 µm/h. During the course of reduction, the solution pH invariably decreases, requiring continuous additions of an alkali hydroxide. The highly alkaline nature of these baths poses difficulties for use with aluminium substrates.

(iv) **Hydrazine baths** – Hydrazine has also been used to produce electroless nickel deposits (Levy 1963; Dini & Coronado 1967). These baths operate in the temperature range of 90–95°C and pH range of 10–11. Their rate of deposition is approximately 12 µm/h. Because of the instability of hydrazine at high temperatures, these baths tend to be very unstable and difficult to control. The deposit contains high amounts of nickel but does not look metallic. The deposit is brittle and highly stressed for practical applications.

**2.2.2b Energy:** Amount of energy or temperature of electroless nickel solutions is one of the important factors affecting the rate of deposition. The rate of deposition is low at temperatures below 65°C, and increases with the increase in temperature. This is true for almost all the systems. Generally the operating temperature is about 90°C, above which the bath tends to become unstable (Boudrand 1994).

**2.2.2c Complexing agents:** One of the difficulties of reduction reactions or chemical plating is the maintenance of the bath composition. As the plating proceeds, continuous lowering of the rate of reduction of nickel occurs. The solutions cannot be replenished

due to the formation of nickel phosphite. If nickel phosphite is precipitated in the bath, the surface quality of coating deteriorates resulting in rough and dark coatings. Moreover, the nickel concentration in the solution also decreases and the bath goes to the verge of total decomposition. Sodium citrate reduces the formation of nickel phosphite and reduces the rate of deposition (Gutziet & London 1954). The ability to form nickel complexes has been attributed to some of the proposed additives like salts of glycolic, succinic or malonic acids, however, these fail to stop the precipitation of nickel phosphite. The best results are obtained when the sodium citrate concentration is about 30 g/l. It helps in checking the coating from becoming porous and dull. Because of the reduction in rate of deposition, accelerators like salts of carbonic acids, soluble fluorides and inhibitors like thiourea can also be added to avoid the total decomposition of the bath. Bi, Pb, Cd and Te additions act as bath stabilisers (Lanzoni et al 1997). Bismuth and Te seem to be less effective than Pb and Cd in bath stabilization. These stabilizers are added in concentrations of only a few parts per million.

### **2.2.3 Factors affecting the coating process**

Bath composition is the major parameter affecting the coating process; however, other factors like pH, temperature, bath loading factor, i.e., the surface area of the substrate also affect coating process in a major way. Variation in nickel salt concentration has no noticeable influence on the rate of reduction of nickel but variation in hypophosphite concentration affects the process considerably. Although increase in hypophosphite concentrations improves the rate of reduction of nickel, extra amounts of reducing agents should not be used as this may cause reduction to take place in the bulk of the solution. The appropriate amount of hypophosphite can be adjusted by observing the bath condition during the course of reaction. Weak hydrogen evolution is an indication of a low concentration of hypophosphite and a vigorous hydrogen evolution indicates excess hypophosphite. Nickel deposits obtained from acid solutions have a very bright and smooth surface; coatings obtained from alkaline solution have a bright surface. As the alkalinity of the solutions increases, the nickel content of the deposit increases or the phosphorus content decreases. Phosphorus may be present as a phosphide or as solid solution. The concentration of nickel salts has slight influence on the rate of deposition.

Large concentrations of nickel salt cause deterioration in the quality of the coatings with the formation of rough deposits. Sulphate and chloride baths are used for depositing amorphous alloys. The results by use of the sulphate baths are found to be systematic while with chloride baths, the results are arbitrary (Cziraki et al 1980). Deposits on aluminium substrates exhibit higher magnetization than on brass substrate. Temperature has a considerable influence on the rate of process. The rate of the process increases with increase in temperature and attains a maximum at about 92<sup>0</sup>C. Beyond this temperature, it becomes difficult to maintain the pH of the solution and, therefore, the quality of the coating deteriorates. As the bath loading increases the rate of deposition increases. There is a critical bath loading factor above which the bath decomposes totally.

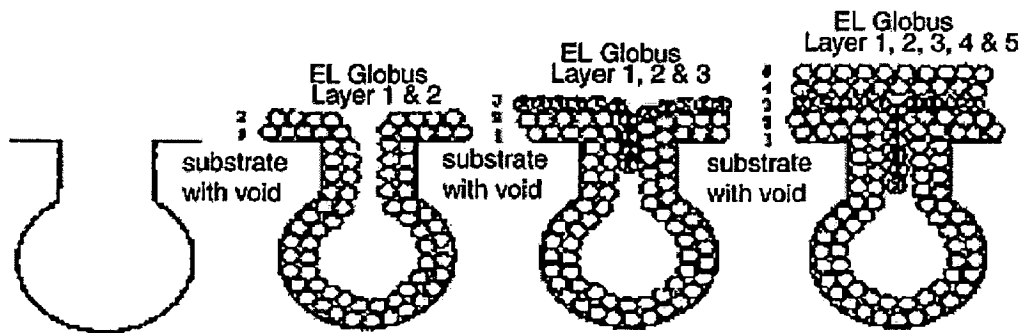


Fig. 2.1 Schematic representation of growth and bonding mechanism of EL coating with the substrate [58].

### 2.3 Electroless composite coating

The co-deposition of particulate matter with electroless nickel coatings dates back to the 1960's (Odekerken 1966). In his pursuit to improve corrosion resistance, of nickel chromium electrodeposits, he used an intermediate layer containing finely divided Al<sub>2</sub>O<sub>3</sub> and PVC particles distributed within a metallic matrix. This intermediate layer was deposited using the electroless coating technique. The initial attempts to produce such deposits were not successful and often resulted in decomposition of the bath. This is not surprising as the methodology pursued for producing the composite coatings were similar to those prevailing in conventional electroplating. Dispersion of finely divided particles increases the surface area loading of the EL plating by 800 times that normally acceptable



for conventional EL plating and this ultimately leads to homogenous decomposition of the bath. However, with the help of suitable stabilizers, EL nickel composite coatings can be prepared[59]. Lately composite coatings of Ni-B with a few other elements have also been reported and are used as light emitting coatings. Successful co-deposition depends on various factors like catalytic or inert nature of particles and their size distribution, bath composition, and the compatibility between dispersoids and metal matrix. Electroless composite coating uses the conventional reduction reaction process with suspensions of particles. Each combination between a certain type of particles and the Ni-P matrix can lead to a new set of properties (Apachitei et al 1998b).

Table 2.1 Different electroless composite coatings developed and primarily referred in literatures

Composite Coating	Reference and Year
Ni-P-Al <sub>2</sub> O <sub>3</sub>	Odekerken, 1966 and Apachitei et al., 1988
Ni-P-SiC	Apachitei et al., 1998; Li,1997 and Grosjean et al., 1997
Ni-P-B <sub>4</sub> C	Ge et al., 1998 and Bozzini et al., 1999
Ni-P-B	Apachitei et al., 1998
Ni-P-C	Cziraki et al., 1980
Ni-P-PTFE	Narayan and Pandey, 1997; Pena-Munoz et al., 1998 and Zhang et al., 1998
Ni-P-MoS <sub>2</sub>	Moonir-Vaghefi et al., 1997

### 2.3.1 Mechanism of particle incorporation

There are two ways to add second phase particles X (ZnO in our case):

**In-Situ-** In this method the precursors that can synthesize X are added to the electroless bath and the synthesis as well as deposition of X takes place.

**Ex-Situ-**In this method the precursors are used to synthesize X outside the bath and are added externally during deposition process so that x is co-deposited along with Ni-P.

The electroless composite coating is formed by the impingement and setting of particles on the surface work piece, and the subsequent envelopment of these particles by the matrix material as it is deposited. There is no molecular bonding between particles and

metal matrix. The mechanism of particle incorporation in electroless Ni-P matrix has received very little attention.

### **2.3.2 Factors influencing particle incorporation**

Several factors influence the incorporation of second phase particles in an electroless Ni-P matrix including particle size and shape, relative density of the particle, particle charge, inertness of the particle, the concentration of particles the plating bath, the method and degree of agitation, the compatibility of the particle with the matrix, and the orientation of particle being plated.

The size of the particles has a definite impact on their incorporation in the electroless Ni-P matrix. In general, it is recommended that particles must be selected with reference to the thickness of the electroless nickel deposit.

Particle shape also plays a vital role in determining their incorporation level. It is generally believed that angular particles will have a greater tendency to hold on the surface upon impingement than round ones. Although better results have also been obtained with spherical particles as in case of alumina. The difference in particle shape also has a bearing on the type of finish of the deposit. Very smooth and very rough surfaces were obtained, respectively, from small rounded particles and large angular particles[59].

## **2.4 Applications of ZnO**

ZnO production is approximately 105 tons per year. Zn is evidently much more available (and less poisonous!) than, e.g., Ga. In the following, we give first a list of a variety of existing applications and then an outlook or vision for future applications, especially in the field of optoelectronics, including junctions.

### **2.4.1 Present applications**

A large fraction of the ZnO is used in the rubber and concrete industries [60]. ZnO is an important additive to the rubber of tires of cars. It has a positive influence on the vulcanization process and it improves considerably the heat conductivity that is crucial to

dissipate the heat produced in the rubber of the tire by the deformation when it rolls along the street. In concrete an admixture of ZnO allows increased processing time and improves the resistance of the concrete against water. Other applications concern medicine or cosmetics. ZnO is used as a UV-blocker in sun lotions or as an additive to human and animal food. Furthermore, it is used as one component of mixed oxide varistors, devices that allow voltage limiting [61].

#### **2.4.2 Future applications:**

Since the surface conductivity of ZnO can be strongly influenced by various gases, it is used as a gas sensor [62]. The pointed tips of single crystals and nanorods (Figs. 3 and 5) result in a strong enhancement of an electric field. Therefore they can be used as field emitters [63].

Due to its wide bandgap, ZnO is transparent in the visible part of the electromagnetic spectrum. Highly n-doped ZnO:Al can therefore be and partly is already used as a transparent conducting oxide (TCO) [64]. The constituents Zn and Al are much cheaper and less poisonous compared to the generally used indium-tin oxide (ITO). One application is as the front contact to solar cells, which avoids the shadow effect necessarily connected with metal finger contacts. Another application is as the front contact of liquid crystal displays [65], still another of ZnO : Al is in the production of energy-saving or heat protecting windows. For the properties of ZnO as a UV-sensitive and solar-blind photo detector see [66] and for its hardness against high-energy radiation see [67]. Furthermore, transparent thin-film transistors (TFT) can be produced with ZnO.

Zinc oxide and ZnO-based materials demonstrate significant antimicrobial activity, as they are non-irritating, and absorb moisture and odours. Moreover, zinc oxide is non-toxic and compatible with skin, making it suitable additive for textile and surfaces that come in contact with humans. The attenuation properties also make ZnO as effective additive for packaging plastics to prevent UV damages. Thermal stability of zinc oxide based materials imparts permanence to their activity and enables these materials to be incorporated into plastics and on surfaces that experience extreme processing or harsh

application environments yet they remain active. Nanoscale zinc oxide offers greater surface area than their bulk counter-parts, which improves product performances, the enhanced surface area of zinc oxide nanoparticles allow for increased interaction with bacteria. This permits using a smaller amount of zinc oxide for the same or improved biostatic behaviour.

## **2.5 Applications of Electroless Ni Coatings**

Electroless Nickel is normally applied for five different applications: coatings used for corrosion resistance, wear resistance, lubricity, solderability, buildup of worn or over machined surfaces. To varying degrees, these properties are utilized by all segments of industry, either separately or in combination. It is commonly used in engineering coating applications where wear resistance, hardness and corrosion protection are required. Applications include oil field valves, rotors, drive shafts, paper handling equipment, fuel rails, and optical surfaces for diamond turning, door knobs, kitchen utensils, bathroom fixtures, electrical/mechanical tools and office equipment. It is also commonly used as a coating in electronics printed circuit board manufacturing. Due to the high hardness of the coating it can be used to salvage worn parts. It is also used extensively in the manufacture of hard disk drives, as a way of providing an atomically smooth coating to the Aluminium disks, the magnetic layers are then deposited on top of this film, usually by Sputtering and finished with protective carbon and lubrication layers; these final two layers protect the underlying magnetic layer (media layer) from damage should the read / write head lose its cushion of air, and contact the surface. Its use in the automotive industry for wear resistance has increased significantly.

### **(a) Petroleum and Chemical Industries**

The petroleum and chemical process industries are the largest users of electroless nickel for corrosion protection. High phosphorus coatings are commonly used to resist corrosion and erosion in aggressive brines, acids and gases. Common applications include valves, chokes, blowout preventers, mud pumps, sucker rod and submergible pumps, pipe, heat

exchangers and separators, packers, safety valves, production tubing[Mallory, G.O., et.al (1980), Agarwala, R.C. and Agarwala, V.(2003)]

#### **(b) Medical, Dental and Pharmaceutical**

Electroless nickel is also used for medical, dental and pharmaceutical equipments because of superior corrosion and wear resistance. Electroless nickel provides almost complete resistance to these environments and frequently allows steel or aluminium to be used instead of more expensive stainless steel.

Typical medical applications are scissors, suture needles, clamps, forceps and hubs for disposable hypodermic needles. In the pharmaceutical industry, extruders, sizing screens, pill sorters and filing equipment are common applications [Mallory, G.O., et.al (1980), Agarwala, R.C. and Agarwala, V.(2003)]

#### **(c) Printing and Textile Industries**

The use of electroless nickel for the cylinders and rolls used in the printing and textile industries has grown greatly during the past several years. The ability of the coating to deposit uniformly allows the cylinder to be machined to size, balanced, and plated without subsequent finishing or grinding. The life of the equipment is also greatly extended by the lubricity and wear resistance of electroless nickel. Other common textile applications include thread guides, fiber feeds, fabric knives, heddles, bobbins, shuttles, rapiers, ratchets, knitting needles and picks [Mallory, G.O., et.al (1980), Agarwala, R.C. and Agarwala, V.(2003)]

#### **(d) Aerospace**

In the aerospace industry, electroless nickel is used to protect the surface of light metals, such as aluminium, from corrosion and wear. It also enhances the appearance of these metals with a polished, stainless steel look. The coating is used on a variety of aircraft parts, including engine components, structural air frame and landing gear pieces, refuelling systems, compressor blades, and servo valves. Its uniform thickness, and its ability to coat the inside of holes and recesses, makes electroless nickel an ideal coating

for welded tanks and complex hydraulic valve and manifold systems [Mallory, G.O., et.al (1980), Agarwala, R.C. and Agarwala, V.(2003)]

#### **(e) Packaging and Handling**

With packaging machinery and food handling equipment, electroless nickel is also used because of its excellent wear and corrosion resistance. The coatings provide an attractive finish and help to ensure the cleanliness of the part. Electroless nickel is used to handle such diverse products as sodium hydroxide, food grade acids and fish oils. Its uniform deposit is especially useful for hydraulic cylinders, worm feeds and extruders, shafts, chain belts and other close fitting parts. Common food handling applications include pneumatic canning machinery, hamburger molds and grills, bun warmers, baking pans, fryers and chocolate molds [Mallory, G.O., et.al (1980), Agarwala, R.C. and Agarwala, V.(2003)]

#### **(f) Mining**

Equipment for mining operations is a growing application for electroless nickel coatings. Mining environments are both very corrosive and abrasive. Mine waters are typically acidic and can cause high rate of attack of unprotected steel. In addition, the dust produced during mining can result in severe erosion. Electroless nickel coatings have been found to withstand these conditions with little attack. Common applications are hydraulic components, framing, cylinder heads for jetting pumps, pipeline connections and tubing, and mine engine components [Mallory, G.O., et.al (1980), Agarwala, R.C. and Agarwala, V.(2003)]

#### **(g) Wood, Pulp and Paper**

Wood handling, pulp and paper equipment operate under conditions of severe corrosion and abrasion. The salt and organic acids present woods can cause high rates of attack on common materials. Electroless nickel coatings provide good protection against these conditions and are presently being used for knife holder cover plates and for abrading plates for wood cutting and chopping machines. Differential pins are also a large application area [Mallory, G.O., et.al (1980), Agarwala, R.C. and Agarwala, V.(2003)]

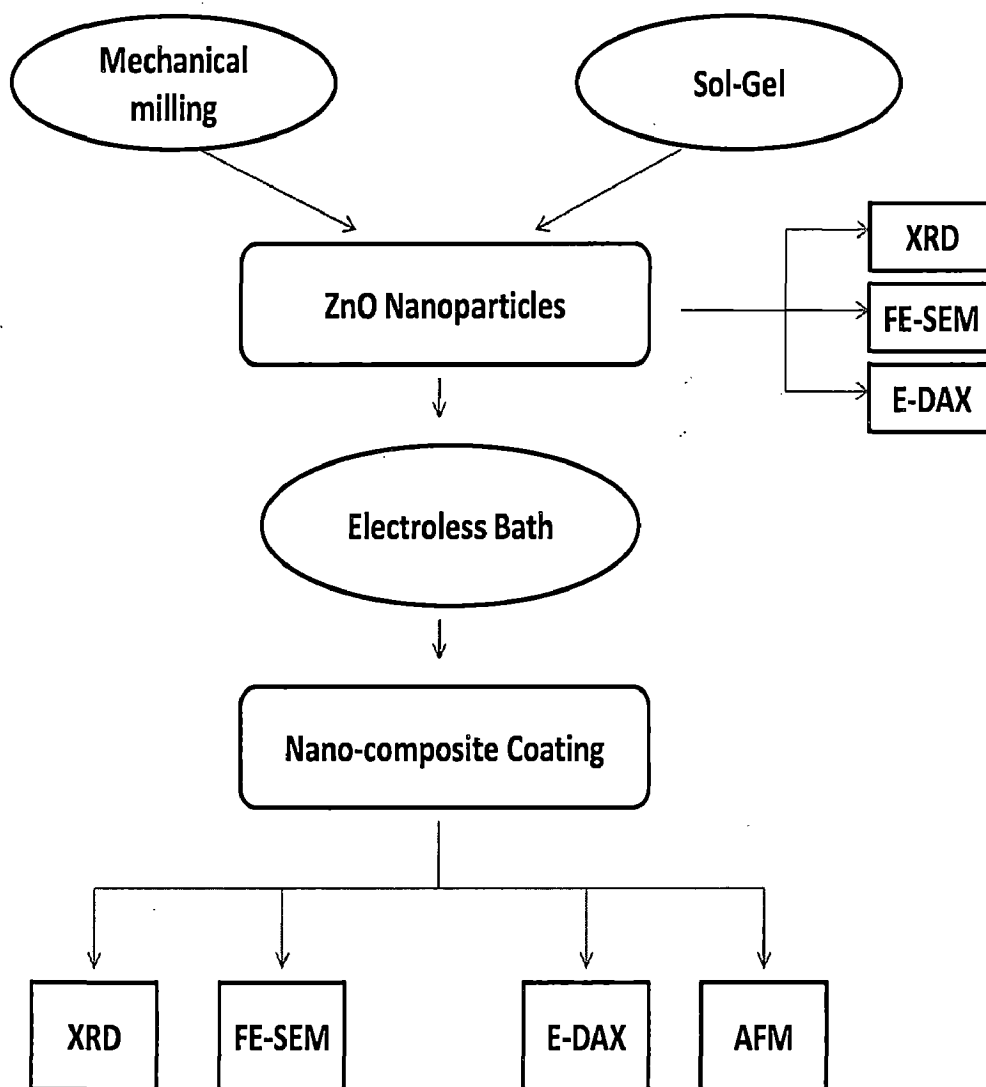
#### **(h) Food Process**

Electroless nickel (most often high phosphorus type) is used for a variety of applications, including evaporators in ice machines, bearings, gears, conveyors and chains. Electroless nickel coatings have replaced expensive stainless steel (or have been used to coat stainless steel), because foodstuffs do not tend to stick readily to them. Also electroless nickel coated components are not as receptive to stress corrosion cracking as stainless steels (many cleaning compounds use chlorides) [Mallory, G.O., et.al (1980), Agarwala, R.C. and Agarwala, V.(2003)]

## CHAPTER 3

### FORMULATION OF PROBLEM

---





ZnO is known for a wide number of applications, to utilize these applications along with the applications of electroless coatings the problem was designed. The aim of this work was to incorporate zinc oxide nanoparticles into coating for the utilisation of its applications, after careful considerations electroless coating was decided for its uniformity, hardness, wear resistance and other advantages as reported in chapter-2. For the synthesis of nanocomposite coatings with zinc oxide as second phase particles, zinc oxide nanoparticles were synthesized first. Physical method was used for its economical production and easy scale up possibility. Mechanical milling was employed using PM-4002 planetary ball mill. Chemical compounds were mixed in desired proportion and milling was done for 45 hours, with withdrawal of samples at equal intervals for characterisation studies. After the synthesis of the nanoparticles their incorporation along with Ni-P was taken up, electroless coating technology was employed for this purpose. Nanocomposite coatings so obtained were later characterised by X-Ray Diffraction studies, FESEM study, AFM study.

## CHAPTER 4

### EXPERIMENTAL WORK

---

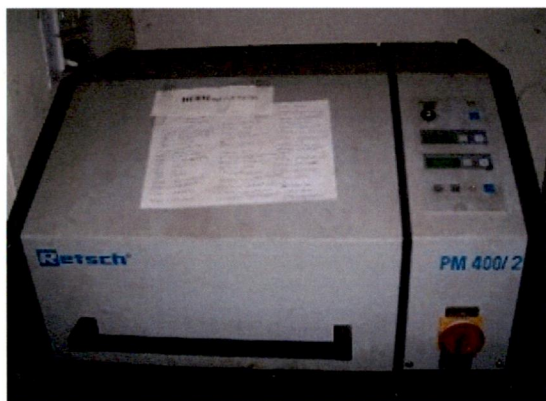
#### 4.1) Materials and Instruments used

##### 4.1.1) Chemical salts and Reagents used

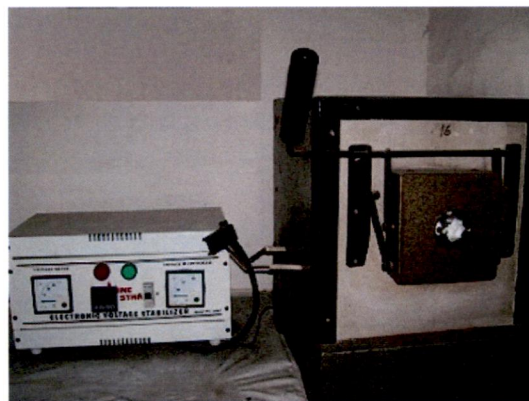
- Zinc Chloride (Himedia)
- Sodium carbonate (Himedia)
- Sodium chloride (Merck)
- Zinc acetate dehydrate (Merck)
- Methanol (Rankem)
- Nickel sulphate (Merck)
- Sodium hypophosphite (Loba Chemie)
- Tri sodium citrate (Merck)
- Ammonium sulphate (Merck)
- Stannous chloride (Merck)
- Palladium chloride (Merck)
- Ammonia (Merck)
- Acetone (Rankem)
- Hydrochloric acid (Rankem)

##### 4.1.2 Instruments and Equipments used

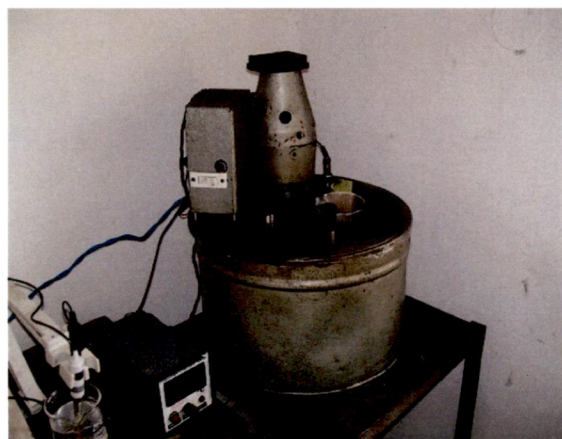
- PM-400/2 High energy planetary ball mill (Fig. 4.1 (a))
- Electric furnace (Fig. 4.1 (b))
- Magnetic stirrer (Make REMI)
- Electroless bath (Fig. 4.1 (c))
- pH meter (Make EUTECH ) (Fig. 4.1 (d))
- Bruker X-8, X-Ray diffraction instrument
- FEI Quanta200f for FESEM and EDAX
- Elix Millipore for Distilled water (Fig. 4.1 (e))



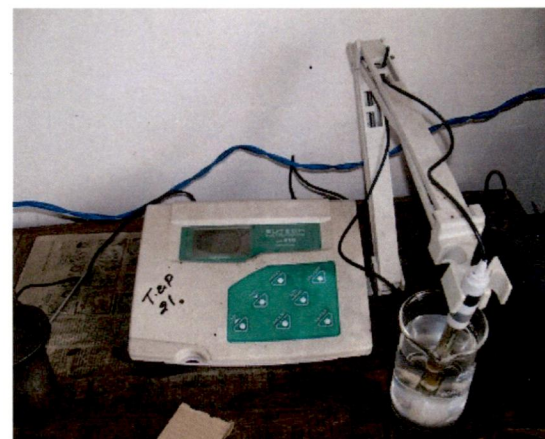
(a)



(b)



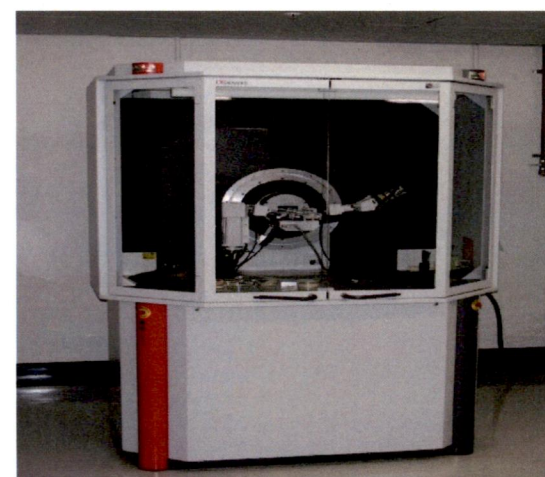
(c)



(d)



(e)



(f)

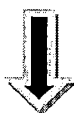
Fig:4.1 Instruments used (a) PM 400/2 High Energy Planetary Ball Mill (b) Electric Furnace (c) Electroless Bath (d) pH Meter (e) Elix Milipore for Distilled water (f) Bruker D-8 Advance

## 4.2 Synthesis of Zinc Oxide Nanoparticles by mechano-chemical synthesis

Initially  $\text{ZnCl}_2$ ,  $\text{Na}_2\text{CO}_3$ ,  $\text{NaCl}$  were taken in molar ratio 1 : 1 : 6



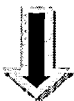
Salts were mixed and put in a stainless steel jar



Balls added in 1:1 weight ratio to the powder, to the jar and place the jar in planetary ball mill PM 400/2



Mixture rotated at 200 rpm



Samples withdrawn at intervals of 5 hours



Characterisation by X-Ray Diffraction on Bruker X-8, FESEM Analysis and EDAX Analysis done on FEI Quanta 200f

### **4.3 Synthesis of Zinc Oxide Nanoparticles by sol-gel method:**

**Initially 0.2 molar solution of Zinc acetate dehydrate and methanol were taken**



**The solution was stirred by magnetic stirrer for 36 hours**



**Solution is kept in oven at 100<sup>0</sup>C for 12 hours**



**After evaporation of solvent powder is heat treated at 400<sup>0</sup>C for 2 hours**



**Characterisation by X-Ray Diffraction on Bruker X-8, FESEM Analysis and EDAX Analysis done on FEI Quanta 200f**

## **4.4 Synthesis of Ni-P-ZnO Nanocomposite electroless coating:**

### **4.4.1 Substrate Preparation and Pre-treatment:**

Substrates in the form of mild steel blocks were meticulously prepared for electroless coatings so as to remove the oxide layer and other adhering material in order to ensure the good adhesion between the substrate and the coating. Samples were polished following the standard method using emery paper up to 4/0 grade before its preparation and pre-treatment.

### **4.4.2 Steps for Surface Preparation:**

Following steps were followed:

- I. Degreasing with an organic solvent (Acetone),
- II. Degreasing with sodium hydroxide,
- III. Etching in dilute hydrochloric acid,
- IV. Washing with distilled water and
- V. Drying

### **4.4.3 Surface Pre-treatment:**

The steps followed in the pre-treatment of the samples for initialisation and sensitization of substrates, are given below:

- I. Dipping in 0.1% stannous chloride,  $\text{SnCl}_2$ , solution for 2 minutes,
- II. Dipping in 0.01% palladium chloride,  $\text{PdCl}_2$ , solution for 1 minute.

All the samples were subjected to thorough rinsing with distilled water and dried after each step mentioned above before proceeding for next step.

### **4.4.4 Bath Composition and Operating Conditions:**

In the light of discussion in chapter 2, sodium hypophosphite was used as the reducing agent in the electroless nickel bath. The bath was periodically stirred so as to keep the bath composition uniform and to prevent the local heating of the bath. Also ammonia solution was added as and when required

Table 4.1 Bath composition and operating conditions

Volume of distilled water	250 ml.
Nickel sulphate	6.25 gm.
Sodium hypophosphite	5 gm.
Tri sodium citrate	22.5 gm.
Ammonium sulphate	12 gm.
Temperature	90 <sup>0</sup> C
pH	8.5-9
ZnO	2 gm.
Coating time	30-60 minutes
pH controlling reagent	Ammonia

#### 4.4.5 Process Details:

Indigenously fabricated set up as shown in fig. 4.2 was used for the synthesis of electroless composite coating.

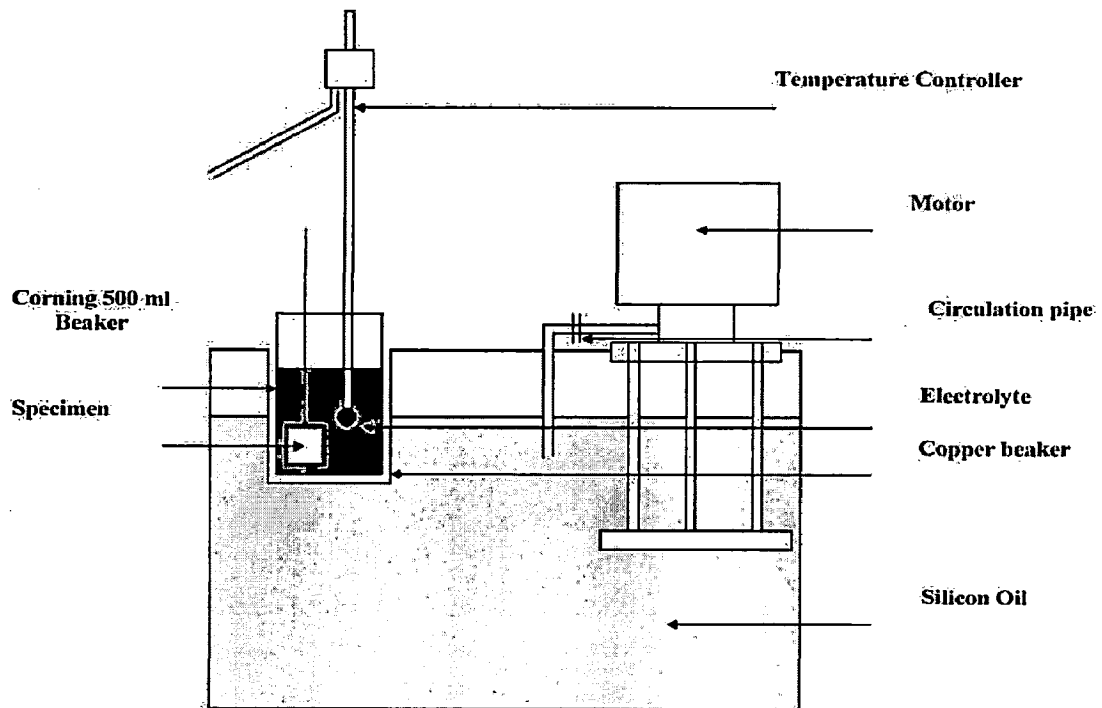


Fig. 4.2 Schematic diagram of the experimental set-up used for EL coating bath[33]:

The prepared electroless bath was placed in the copper beaker and heated electrically in the oil bath. Due care was taken in maintaining the temperature and pH of the bath solution by using temperature controller and pH meter respectively. Before immersing the substrate into the bath, it was assured that the bath temperature has stabilized to the desired value and pH properly adjusted. The pH of the bath was continuously monitored and intermittently stirred during the coating process. The stirring was used to avoid the local variations in pH and temperature of the bath. After successful coatings, the samples were washed with distilled water and dried in air.

#### **4.4.6 Procedure:**

- I. Distilled water was taken in a beaker and kept in the electroless bath
- II. On attainment of desired temperature salts were added
- III. pH of the bath was checked and maintained by adding ammonia
- IV. Pre-treated substrate was added in the bath
- V. After an initial layer of Ni-P was deposited on the substrate the ZnO nanoparticles were added to the bath
- VI. Bath was stirred continuously
- VII. After 30 minutes substrate was removed, washed and dried
- VIII. Heat treatment of coated substrate at 400<sup>0</sup>C for 1 hr. was done.

#### **4.4.7 Precautions**

- NaCl is removed from the powder mixture containing zinc oxide after repetitive washing which must be confirmed after regular washing steps.
- The final output is very small compared to the initial input of salts, hence the amount of salts to be milled initially should be decided after utmost consideration.
- The electroless nickel-phosphorus coating process is very sensitive to various parameters such as temperature, pH. Because with little variation in temperature and pH; we get different phosphorus content in Ni-P deposit, which greatly effect physical and chemical properties of deposit.
- Temperature and pH should be monitored regularly as they influence the uniformity and rate of coating process, any deviation from optimum pH reached



after careful experimentation should be corrected by addition of acid or base as the need may be.

- The salts to be utilised should be free from heavy metals which may hinder the coating process.
- The beakers and others equipments used should be washed carefully as presence of other materials may be disastrous for the reaction.

## **4.5 Characterisation techniques**

### **4.5.1 X-Ray Diffraction Analysis**

X-ray powder diffraction (XRD) is a rapid analytical, non-destructive technique primarily used for phase identification of a crystalline material and can provide information on unit cell dimensions, chemical composition, and physical properties of materials. This technique is based on observing the scattered intensity of an X-ray beam hitting a sample as a function of incident and scattered angle, polarization, and wavelength or energy. Computer analysis of the peak positions and intensities associated with this pattern enables qualitative analysis, lattice constant determination and/or stress determination of the sample. Qualitative analysis may be conducted on the basis of peak height or peak area. The peak angles and profiles may be used to determine particle diameters and degree of crystallization, and are useful in conducting precise X-ray structural analysis. The identification of single or multiple phases in an unknown sample is the main application of X-ray powder diffractometry.

When a monochromatic X-ray beam with wavelength  $\lambda$  is projected onto a crystalline material at an angle  $\theta$ , diffraction occurs only when the distance traveled by the rays reflected from successive planes differs by a complete number  $n$  of wavelengths.

#### **Bragg's Law**

By varying the angle  $\theta$ , the Bragg's Law conditions are satisfied by different d-spacings in polycrystalline materials. Plotting the angular positions and intensities of the resultant diffracted peaks of radiation produces a pattern, which is characteristic of the

sample. Where a mixture of different phases is present, the resultant diffractogram is formed by addition of the individual patterns. The diffraction data is compared against a database maintained by International Centre for Diffraction Data.

X-ray diffractometers consist of three basic elements: an X-ray tube, a sample holder, and an X-ray detector. X-rays are generated in a cathode ray tube by heating a filament to produce electrons, accelerating the electrons toward a target by applying a voltage, and bombarding the target material with electrons. When electrons have sufficient energy to dislodge inner shell electrons of the target material, characteristic X-ray spectra are produced. These spectra consist of several components, the most common being  $K_{\alpha}$  and  $K_{\beta}$ .  $K_{\alpha}$  consists, in part, of  $K_{\alpha 1}$  and  $K_{\alpha 2}$ .

Copper is the most common target material for single-crystal diffraction, with Cu  $K_{\alpha}$  radiation = 0.5418Å. These X-rays are collimated and directed onto the sample. As the sample and detector are rotated, the intensity of the reflected X-rays is recorded. When the geometry of the incident X-rays impinging the sample satisfies the Bragg Equation, constructive interference occurs and a peak in intensity occurs. A detector records and processes this X-ray signal and converts the signal to a count rate which is then output to a device such as a printer or computer monitor. The geometry of an X-ray diffractometer is such that the sample rotates in the path of the collimated X-ray beam at an angle  $\theta$  while the X-ray detector is mounted on an arm to collect the diffracted X-rays and rotates at an angle of  $2\theta$ . The instrument used to maintain the angle and rotate the sample is termed a goniometer.

#### **4.5.2 FESEM Analysis**

FESEM stands for Field emission scanning electron microscope. The FESEM is a microscope that uses electrons instead of light to form an image. Since their development in the early 1950's, scanning electron microscopes have developed new areas of study in the medical and physical science communities. The FESEM has allowed researchers to examine a much bigger variety of specimens.

The scanning electron microscope has many advantages over traditional microscopes. The FESEM has a large depth of field, which allows more of a specimen to be in focus at

one time. The FESEM also has much higher resolution, so closely spaced specimens can be magnified at much higher levels. Because the FESEM uses electromagnets rather than lenses, the researcher has much more control in the degree of magnification. All of these advantages, as well as the actual strikingly clear images, make the scanning electron microscope one of the most useful instruments in research today.

**Various parts of FESEM:** The sample is fixed with conductive tape on a metallic sample block. Non-conductive specimens are coated with a nanometer thin-layer of metal to facilitate emission and flow of electron in the surface. The metal block is crewed on a sample holder and positioned in the pre-vacuum chamber, an intermediate chamber with a front and a rear lid. This chamber acts as a lock. When the vacuum in this space is low enough the shutter to the high vacuum (lowest pressure) is opened and the object is shifted with a long rod into the object chamber on a rails just under the column. In order to ease the positioning a one can observe the inner view of the object chamber with an infra red camera. The object chamber is the place where the sample is irradiated by the electron beam. The position of the sample stage can be adjusted in height (z-navigation) and horizontally (x-y navigation). The topographical scanning electron imaging requires a secondary electrons detector, like in a normal SEM there is a control panel, a monitor for the operation of the device and one showing the SE images. A separate EDS detector allows one to capture the X-ray scanning and there is another back-scattered electron detector. In this chamber in the heart of the electron microscope the vacuum is extremely low:  $10^{-6}$  mBar (thus 1:1.000.000.000 the normal atmospheric pressure; vacuum display = 16; around the electron gun the vacuum is even two orders of magnitude lower). The need for such extreme vacuum is that collision of bombarding electrons from the beam with gas molecules in the column would result in heat production. Cooling and supply of electric power are required in order to maintain this extreme vacuum.

Under vacuum, electrons generated by a Field Emission Source are accelerated in a field gradient. The beam passes through Electromagnetic Lenses, focussing onto the specimen. As result of this bombardment different types of electrons are emitted from the specimen. A detector catches the secondary electrons and an image of the sample surface is

constructed by comparing the intensity of these secondary electrons to the scanning primary electron beam. Finally the image is displayed on a monitor.

In SEM the image is formed from secondary electrons that have been dislocated at the surface of the scanned sample by bombarding primary electrons from the electron gun. Those ejected electrons are captured by a detector and the information is converted into an electric signal, amplified and digitalized. The result is a topographical image of the surface of the object, e.g. the surface of a metal coating or lamellae of fish gills (see example here below). Besides secondary electrons, radiation (in particular X-rays and cathodoluminescence in typical samples) as well as back-scattered and so-called Auger electrons with an own energy level are produced upon interaction of atoms in the surface layer of the sample with the primary electron beam. These emission signals, which contain information among others on the element composition of the upper layer, can be received by selected detectors, as is the case in EDAX microscopes for example, and combined with the topographical image.

Besides, there are scanning electron microscopes which are equipped with EDS (Energy Dispersed Spectroscopy) or EDAX (Energy-Dispersed Analysis of X-rays) detectors that capture the emitted X-ray. With such instruments it is possible to determine which elements are present in the surface layer of the sample (at a depth in the micrometer range) and where these elements are present ("mapping technique"). This particular microscope also allows one to capture directly reflected electrons, the so-called back scattered electrons, from which one can obtain a global appreciation whether one or several elements are present in the surface layer of the sample. Also the so-called Auger electrons, which are emitted just under the surface, provide information about the nature of the atoms in the sample.

**SAMPLE PREPARATION FOR FESEM:** Because the SEM utilizes vacuum conditions and uses electrons to form an image, special preparations must be done to the sample. All water must be removed from the samples because the water would vaporize in the vacuum. All metals are conductive and require no preparation before being used.

All non-metals need to be made conductive by covering the sample with a thin layer of conductive material. This is done by using a device called a "sputter coater."

The sputter coater uses an electric field and argon gas. The sample is placed in a small chamber that is at a vacuum. Argon gas and an electric field cause an electron to be removed from the argon, making the atoms positively charged. The argon ions then become attracted to a negatively charged gold foil. The argon ions knock gold atoms from the surface of the gold foil. These gold atoms fall and settle onto the surface of the sample producing a thin gold coating.

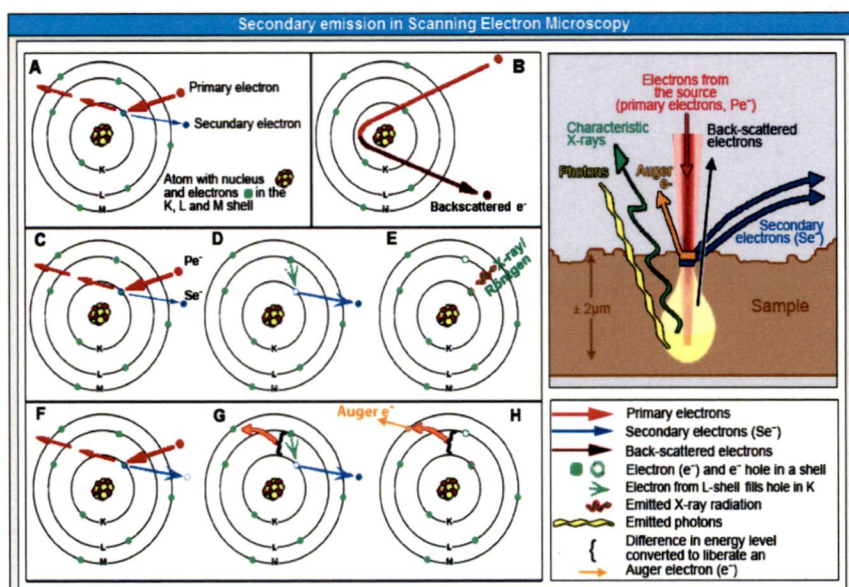


Fig. 4.3 Emissions in SEM

**A:** The bombarding electrons (=primary electrons) can penetrate in the electron shells of the atoms composing the surface of the sample. The energy (negative charge, mass, velocity) of these incident electrons can be converted to eject local electrons, so-called secondary electrons, from the shells of the atoms in the surface of the specimen. This information can be utilized to reconstruct a detailed topographical image of the sample (SEI = Secondary Electrons Imaging). The final image looks like a shadow-cast photograph of the surface of the sample. This record of the morphology is the best-known application of a scanning electron microscope.

**B:** Primary electron can also be reflected by atoms at about 10-100 nanometre depth at the surface. These so-called "back-scatter" conserve their energy at incidence, but their

direction of propagation has been modified upon interaction. One can obtain a rough representation whether the surface of the sample is constituted of a single or multiple elements.

**C, D, E:** at the surface of the sample electrons in the deeper electron shells (shell K in **C**) can be ejected by primary electrons (Pe-indicated in red), resulting in an electron hole. When this lower-shell position is filled by an electron from a higher shell (green arrow in **D**) energy is released. This can be as light (photons; the phenomenon is also called cathode luminescence) or as X-ray. Because each element emits an own characteristic energy value, the elements present in the micrometer range depth of the sample can be determined. See example here below.

**F, G, H:** another phenomenon is that the energy released upon filling a hole in the K shell by an electron from the L shell is used to expulse an electron from the external M shell: a so-called Auger electron. The released energy is characteristic for the type of atom. Auger electrons are produced in the outermost surface layer (at nanometer depth) of the sample.

#### **4.5.3 EDAX Analysis**

Energy dispersive X-ray spectroscopy (EDS) is an analytical technique used for the elemental analysis or chemical characterization of a sample. It is one of the variants of XRF. As a type of spectroscopy, it relies on the investigation of a sample through interactions between electromagnetic radiation and matter, analyzing x-rays emitted by the matter in response to being hit with charged particles. Its characterization capabilities are due in large part to the fundamental principle that each element has a unique atomic structure allowing x-rays that are characteristic of an element's atomic structure to be identified uniquely from each other.

To stimulate the emission of characteristic X-rays from a specimen, a high energy beam of charged particles such as electrons or protons , or a beam of X-rays, is focused into the sample being studied. At rest, an atom within the sample contains ground state (or unexcited) electrons in discrete energy levels or electron shells bound to the nucleus. The incident beam may excite an electron in an inner shell, ejecting it from the shell while

creating an electron hole where the electron was. An electron from an outer, higher-energy shell then fills the hole, and the difference in energy between the higher-energy shell and the lower energy shell may be released in the form of an X-ray. The number and energy of the X-rays emitted from a specimen can be measured by an energy dispersive spectrometer. As the energy of the X-rays is characteristic of the difference in energy between the two shells, and of the atomic structure of the element from which they were emitted, this allows the elemental composition of the specimen to be measured.

#### **4.5.4 AFM Analysis**

The AFM is a form of scanning probe microscope developed in the mid 1980s. It works by scanning an extremely fine probe on the end of a cantilever across the surface of a material, profiling the surface by measuring the deflection of the cantilever. This allows a 3D profile of the surface to be produced at magnifications over one million times, giving much more topographical information than optical or scanning electron microscopes. Its limitation is that the surface to be observed needs to be very flat or the tip will crash into the 'hills' as it is scanned.

The microscope can run in two modes, contact and close contact. Contact mode scans the probe across the surface, keeping a constant force between tip and sample, maintained by a feedback control. The amount of movement required to keep the constant force is then used to create the image. Close contact mode, often called tapping mode, uses a vibrating cantilever. Simple height data can be obtained from the changes in Z-axis displacement, but phase data can also be obtained. There is a phase difference between the measured signal and the drive signal, caused by interactions between probe and material. A 'phase image' can be formed using this data, which will indicate regions of different composition and/or phase in the material.

**Operating Principle:** The AFM consists of a cantilever with a sharp tip (probe) at its end that is used to scan the specimen surface. The cantilever is typically silicon or silicon with a tip radius of curvature on the order of nanometers. When the tip is brought into proximity of a sample surface, forces between the tip and the sample lead to a deflection of the cantilever according to Hooke's law. Depending on the situation, forces

that are measured in AFM include mechanical contact force, van der Waals forces, capillary forces, chemical bonding, electrostatic forces, magnetic forces (see magnetic force microscope, MFM), Casimir forces, solvation forces, etc. Along with force, additional quantities may simultaneously be measured through the use of specialized types of probe (see scanning thermal microscopy, photo thermal, etc.). Typically, the deflection is measured using a laser spot reflected from the top surface of the cantilever into an array of photodiodes. Other methods that are used include optical interferometry, capacitive sensing or piezoresistive AFM cantilevers. These cantilevers are fabricated with piezoresistive elements that act as a strain. Using a Wheatstone bridge, strain in the AFM cantilever due to deflection can be measured, but this method is not as sensitive as laser deflection or interferometry.

If the tip was scanned at a constant height, a risk would exist that the tip collides with the surface, causing damage. Hence, in most cases a feedback mechanism is employed to adjust the tip-to-sample distance to maintain a constant force between the tip and the sample. Traditionally, the sample is mounted on a piezoelectric tube that can move the sample in the z direction for maintaining a constant force, and the x and y directions for scanning the sample. Alternatively a 'tripod' configuration of three piezo crystals may be employed, with each responsible for scanning in the x,y and z directions. This eliminates some of the distortion effects seen with a tube scanner. In newer designs, the tip is mounted on a vertical piezo scanner while the sample is being scanned in X and Y using another piezo block. The resulting map of the area  $s = f(x,y)$  represents the topography of the sample.

The AFM can be operated in a number of modes, depending on the application. In general, possible imaging modes are divided into static (also called contact) modes and a variety of dynamic (or non-contact) modes where the cantilever is vibrated.



## CHAPTER 5

### RESULTS AND DISCUSSION

---

#### 5.1 Characterisation of ZnO powders

##### 5.1.1 Zinc oxide prepared through physical method

##### 5.1.1.1 X-Ray Diffraction results

Sample Used: 6

Condition: Initial Mixture, Milled for 15, 35, 45 hours

Heated at 600<sup>0</sup>C for 4 hours, Washed with deionised water

Model: Bruker XDS

Range: 5<sup>0</sup> - 120<sup>0</sup>

Target: Copper

To study the different phases coming up X-Ray Diffraction studies of the powder mixture were done. Samples were withdrawn at different time intervals, The X-Ray Diffraction pattern so obtained was:

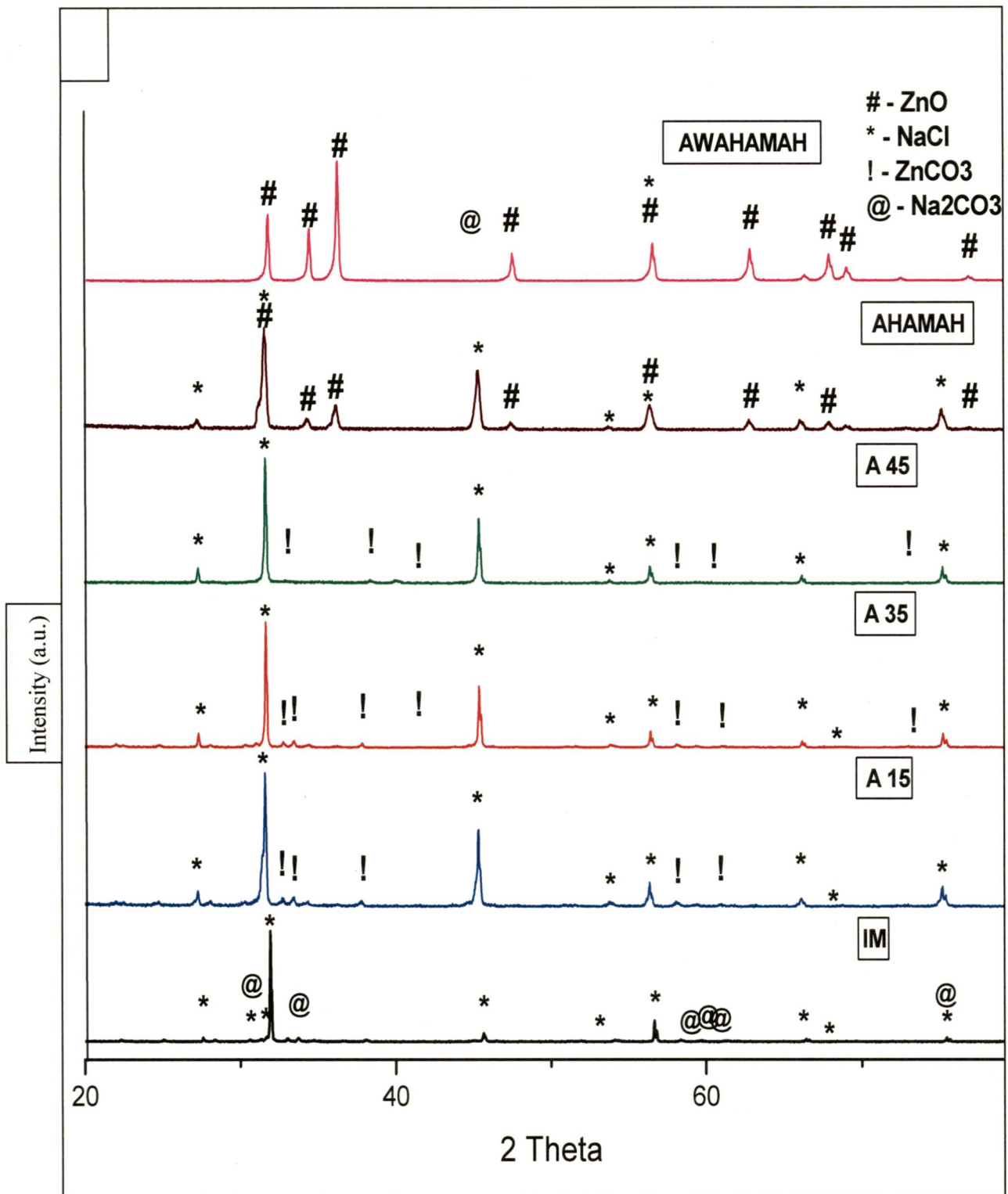
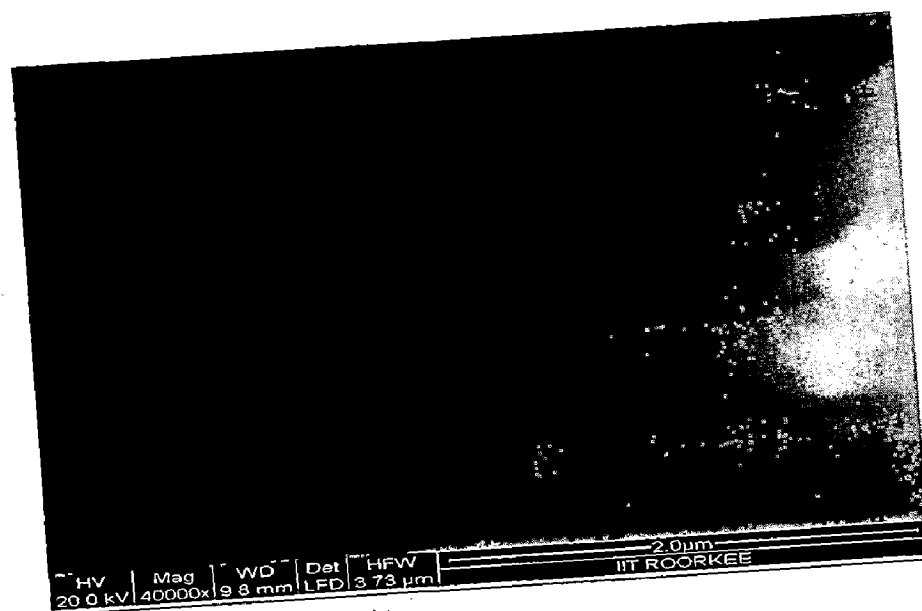


Fig: 5.1 X-Ray Diffraction pattern of powder mixture; (a) Initial mixture; (b) After 15 hours milling; (c) After 35 hours milling; (d) After 45 hours milling; (e) After heating 45 hours milled sample at 600°C for 4 hours and (f) After washing heated sample

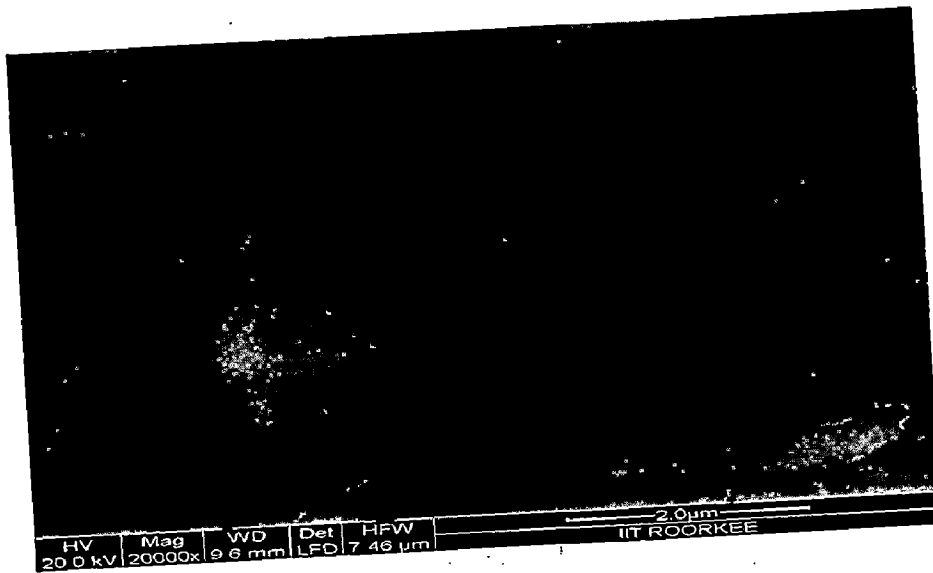
The X-Ray Diffraction pattern shows changes in peaks with time duration showing the occurrence of solid state reaction inside the mill, The new peaks coming up after heating treatment correspond to the peaks of Zinc Oxide. The peaks disappearing after washing step were that of NaCl. The crystallite size is calculated using De-bye Schrer formula, Crystallite size =  $9\lambda / B \cos\theta$ . Where  $\lambda$  is the wavelength of incident light,  $\theta$  is the diffraction angle, and B is the width of the peak at half maximum intensity. The crystallite size found out was 60 nm.

### 5.1.1.2 FE-SEM Results

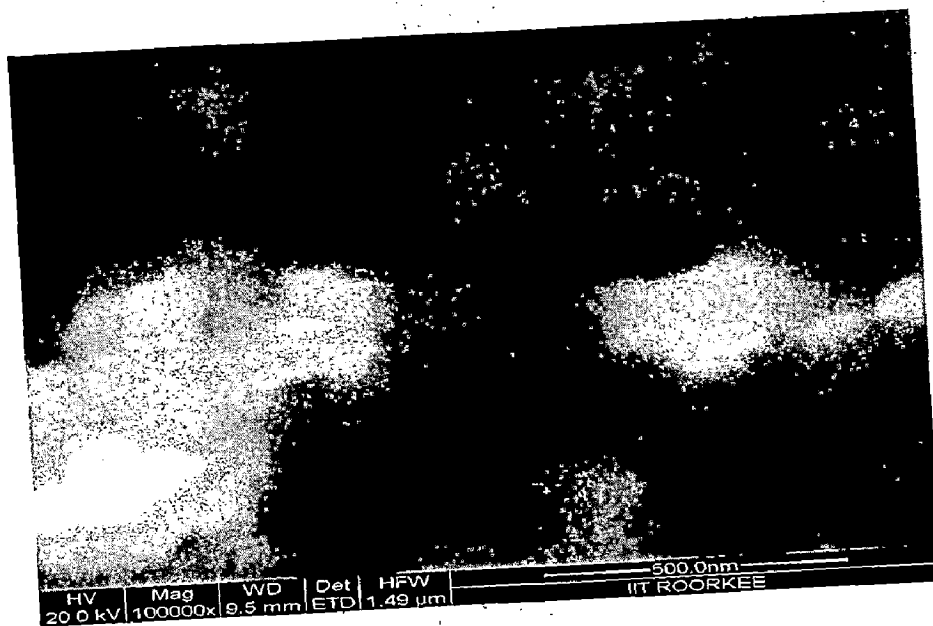
To study the morphology of the particles coming up FE-SEM study of the samples milled for 25 hours and 45 hours was done. FE-SEM Analysis shows the average crystallite size after 45 hours milling is approximately 150 nm. Hence, size is reducing with increase in time of milling. Finally after heating the sample at 600°C and then washing it with De-ionised water we get ZnO nanoparticles of size 50-60 nm. The results of FE-SEM are illustrated down in Fig. 5.2(a-c)



(a)



(b)



(c)

Fig:5.2 (a) FE-SEM image of 25 hours milled sample; (b) FE-SEM image of 45 hours milled sample at 20000x magnification and (c) FE-SEM image of 45 hours milled sample heated at 600°C, after washing with De-ionised water at 100000x magnification

## 5.1.2 Zinc oxide prepared through chemical method

### 5.1.2.1 X-Ray Diffraction results

The X-Ray Diffraction results obtained after analysis of powder confirms the formation of ZnO with the d values of peaks matching with those given in JCPDS. The X-Ray Diffraction pattern so obtained is as given in Fig. 5.3

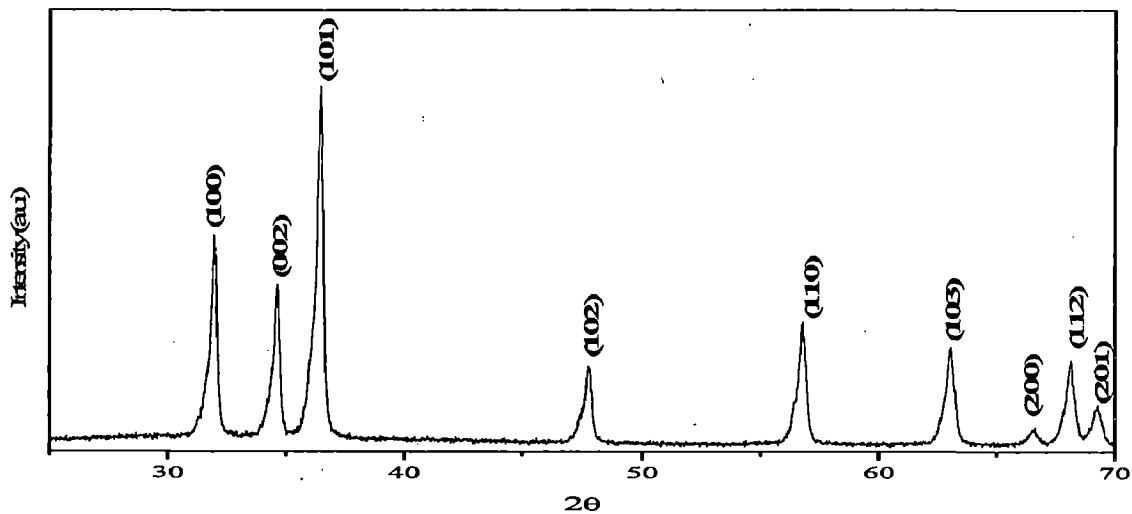


Fig. 5.3 X-Ray Diffraction pattern of Zinc oxide prepared through sol-gel method

The crystallite size is calculated using Debye Scherrer formula,  $\text{crystallite size} = \frac{9\lambda}{B \cos\theta}$ . Where  $\lambda$  is the wavelength of incident light,  $\theta$  is the diffraction angle, and B is the width of the peak at half maximum intensity. The crystallite size found out was 20 nm.

### 5.1.2.2 FESEM results

The surface morphology of the particles coming up were studied using FE-SEM the result obtained for zinc oxide after heating at 400<sup>0</sup>C for 2 hours is as depicted in Fig. 5.4

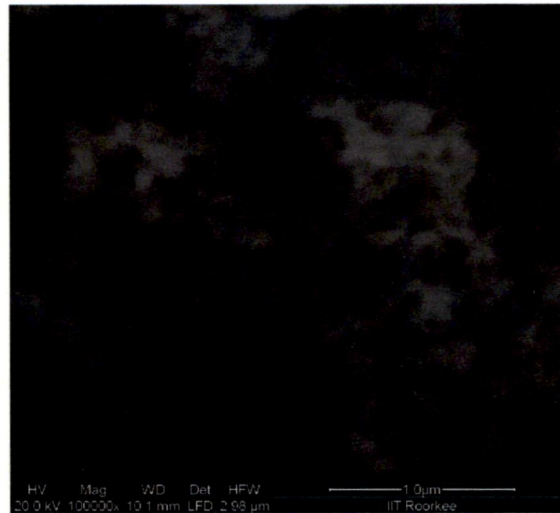


Fig.5.4 FE-SEM of Zinc oxide prepared through sol-gel route

### 5.1.2.3 EDAX Analysis

To study the elemental composition EDAX analysis was done, the results are as shown in fig. 5.5 and table 5.1

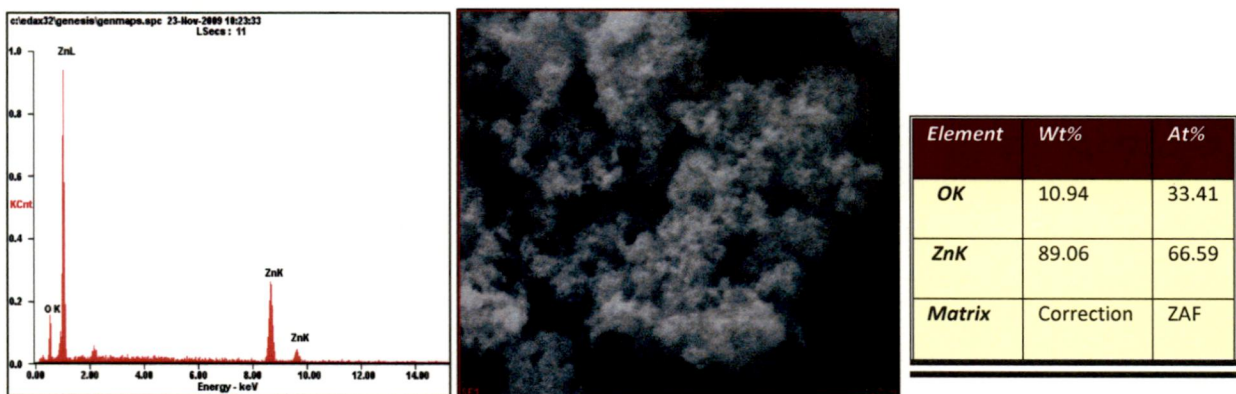


Fig. 5.5 EDAX pattern of Zinc oxide prepared through sol-gel method

## **5.2 Characterisation of Nanocomposite coating**

### **5.2.1 X-Ray Diffraction results**

To study the various phases coming up the X-Ray Diffraction studies of Initial Mild steel substrate, Ni-P coated substrate, substrate coated with Ni-P-ZnO, substrate coated with Ni-P-ZnO followed by heat treatment at 400<sup>0</sup>C for 1 hour. The X-Ray Diffraction results so obtained are as under:

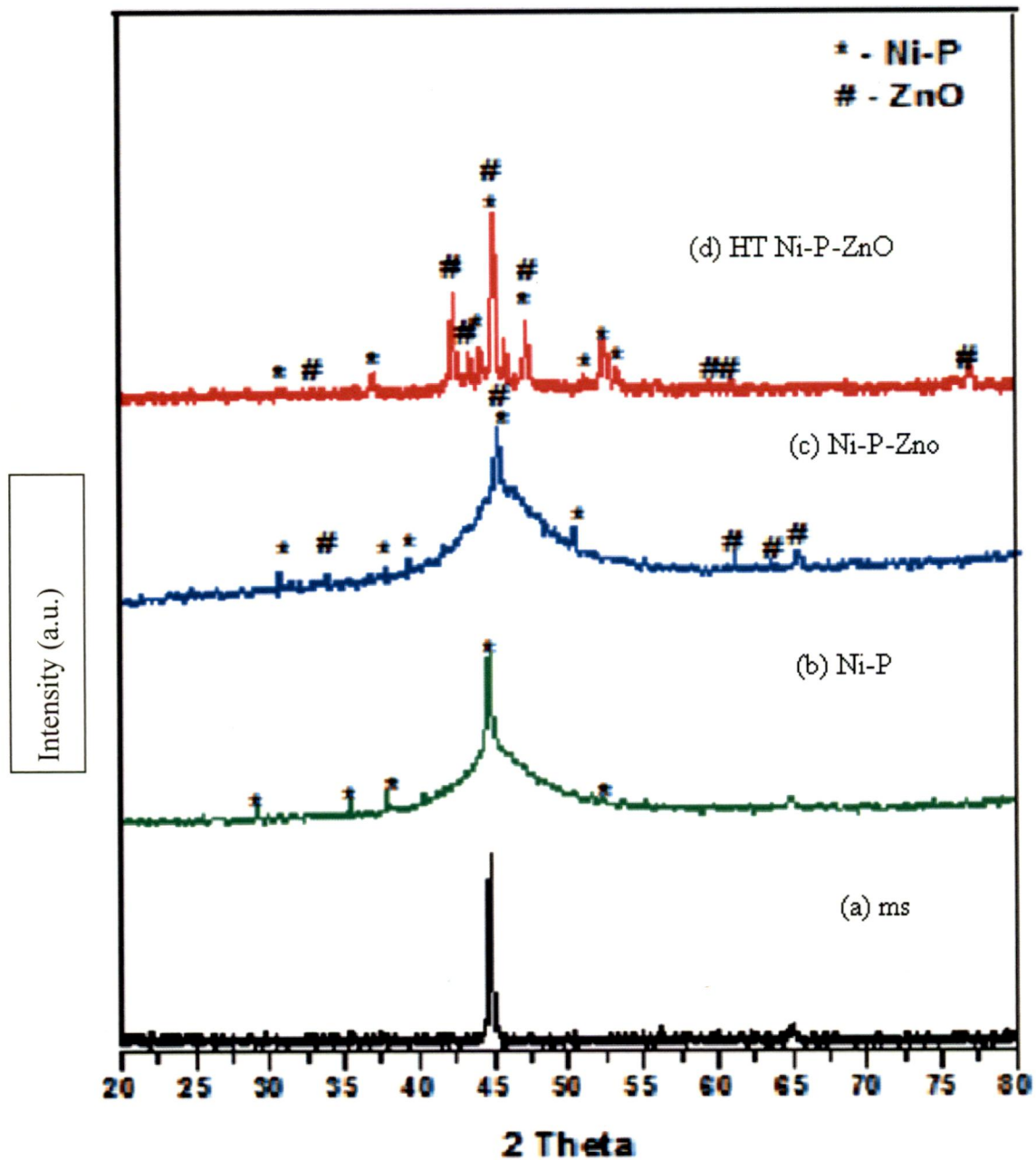


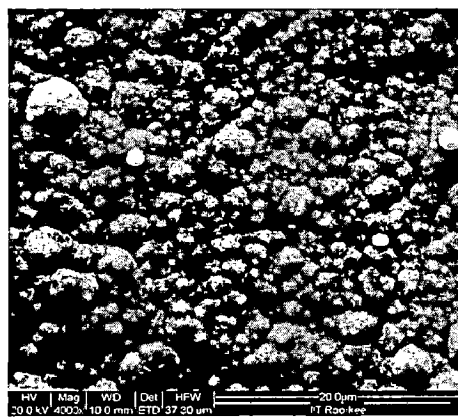
Fig. 5.6 X-Ray Diffraction pattern of Synthesis steps of Nano-composite coating (a) mild steel substrate;(b) Ni-P coated sample;(c) Ni-P-ZnO coated sample and (d) Ni-P-ZnO coated sample after heat treatment.

The crystallite size of incorporated ZnO nanoparticles is calculated using De-bye Schrer formula,  $\text{crystallite size} = 0.9\lambda / B \cos\theta$ . Where  $\lambda$  is the wavelength of incident light,  $\theta$  is the diffraction angle, and B is the width of the peak at half maximum intensity. The crystallite size found out was 100 nm.

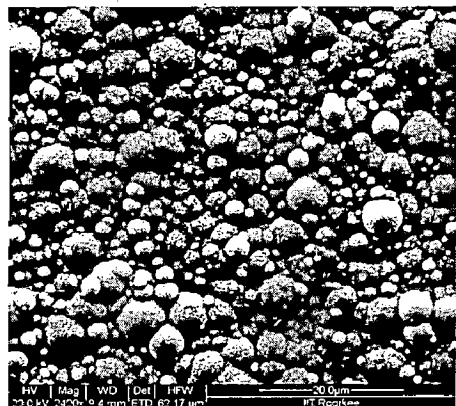


### 5.2.2 FE-SEM analysis

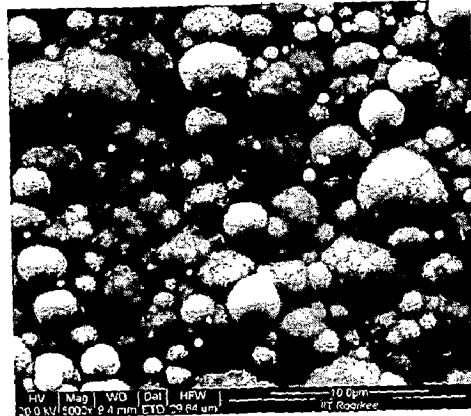
FE-SEM analysis of mild steel sample coated with Ni-P, nanocomposite coating containing ZnO as third phase particles in the matrix of Ni-P, nanocomposite coating heat treated at 400<sup>0</sup>C for one hour. The SEM results so obtained are given in Fig.5.7 (a-e):



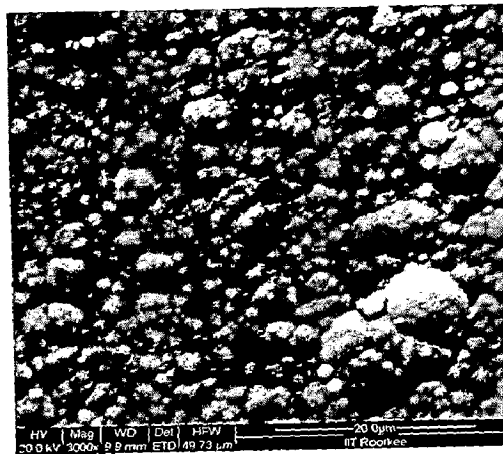
(a)



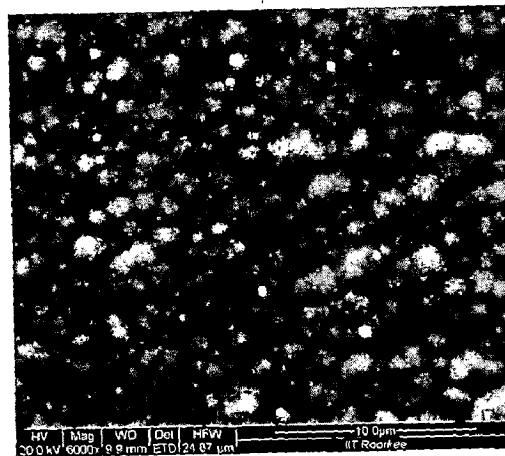
(b)



(c)



(d)

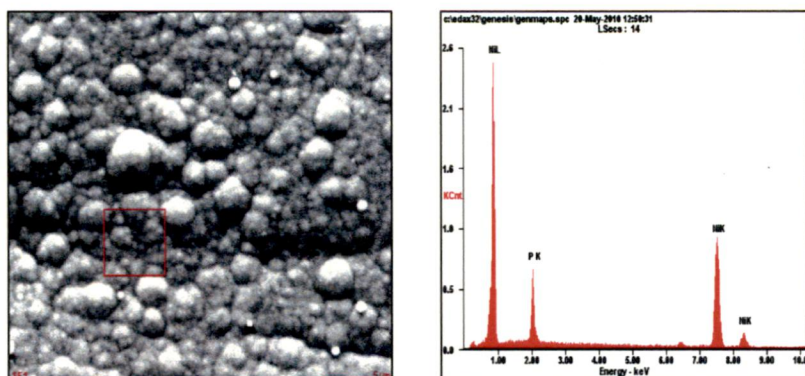


(e)

Fig. 5.7 (a) FE-SEM of sample coated with Ni-P (b,c) FE-SEM of sample coated with Ni-P-ZnO (d and e) FE-SEM of sample coated with Ni-P-ZnO followed by heat treatment

### 5.2.3 EDAX Analysis:

To study the elemental composition EDAX analysis of mild steel sample coated with Ni-P, nanocomposite coating containing ZnO as third phase particles in the matrix of Ni-P, nanocomposite coating heat treated at 400<sup>0</sup>C for one hour was done. The EDAX results so obtained are given in Fig. 5.8 (a-c) and table 5.2 (a-c):

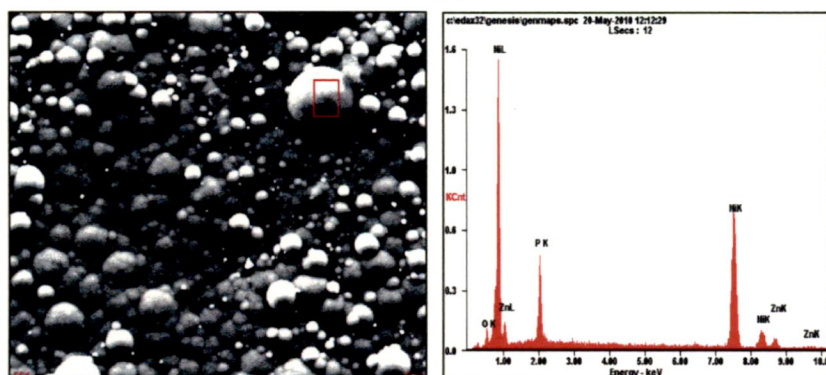


(a)

Table 5.2(a)

Element	WT%	At%
PK	11.26	19.39
NiK	88.74	80.61
Matrix	Correction	ZAF

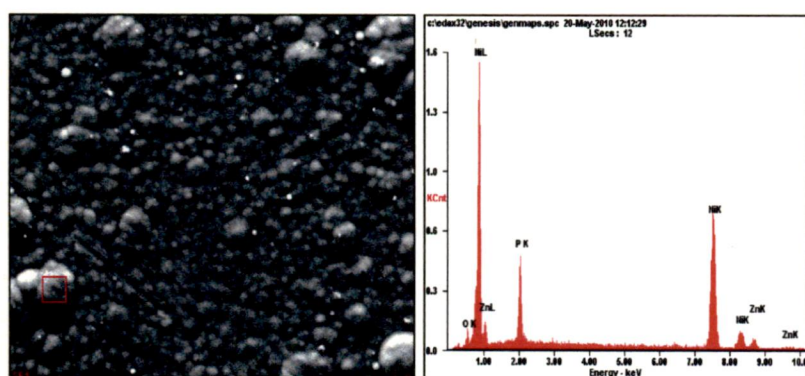
Table 5.2(b)



(b)

Element	WT%	At%
OK	02.72	08.38
PK	14.35	22.81
NiK	74.45	62.43
ZnK	08.47	06.38
Matrix	Correction	ZAF

Table 5.2(c)



Element	WT%	At%
OK	02.04	06.47
PK	12.44	20.41
NiK	75.61	65.42
ZnK	09.92	07.71
Matrix	Correction	ZAF

Fig: 5.8 EDAX of sample coated with (a) Ni-P;(b) Ni-P-ZnO and (c) Ni-P-ZnO after heat treatment

### 5.2.4 AFM Analysis

To study the topography of coating AFM analysis of mild steel sample coated with Ni-P, Nanocomposite coating containing ZnO as third phase particles in the matrix of Ni-P, Nanocomposite coating heat treated at 400<sup>0</sup>C for one hour was done. The AFM results so obtained are given in fig. 5.9 (a-c) and table 5.3 (a-c):

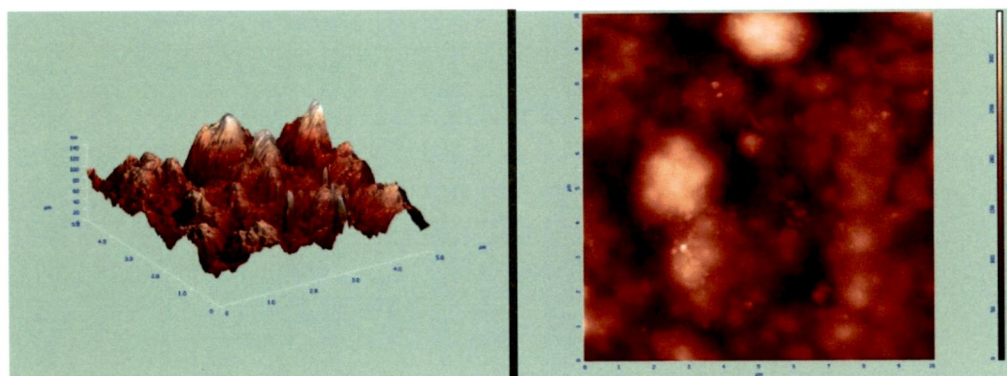
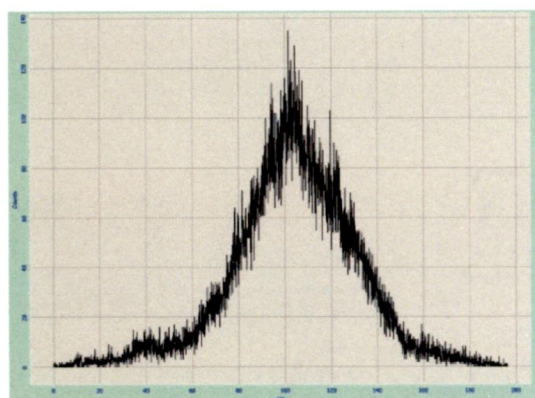


Table 5.3(b) AFM measurements of sample coated with Ni-P



RMS(Roughness)	7 nm
Particle Size	25 nm
Grains	100

(a)

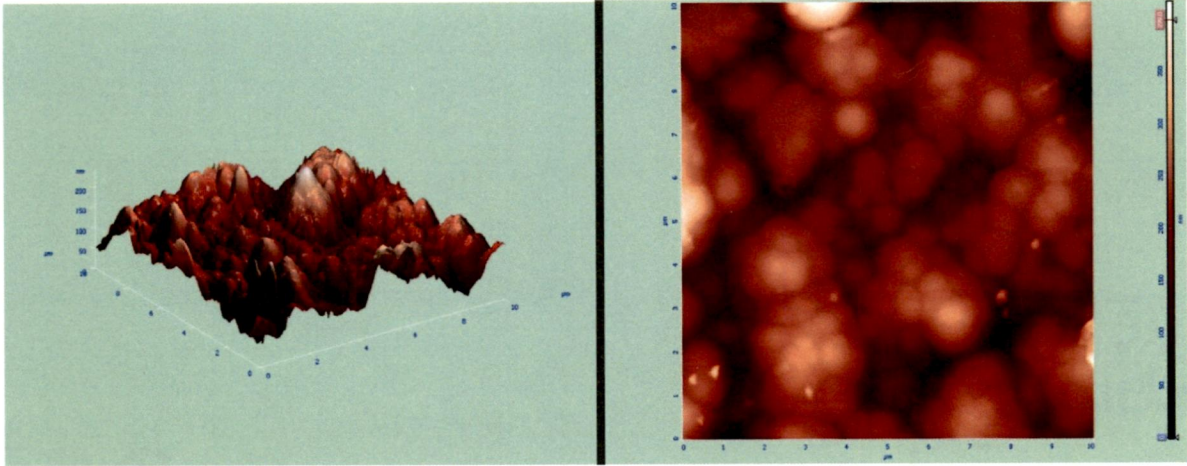
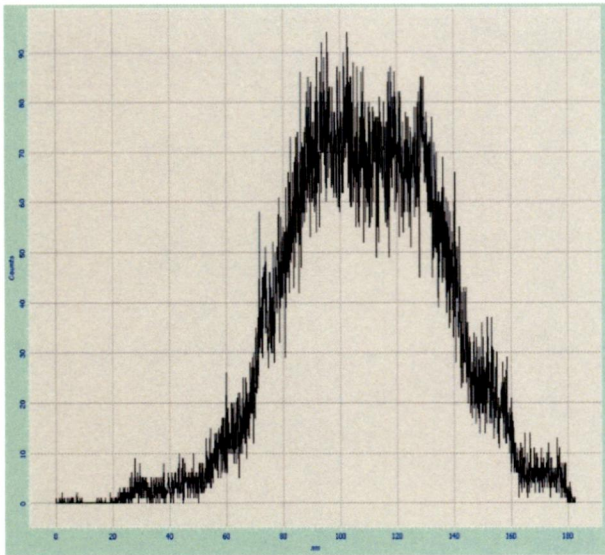


Table 5.3(b) AFM measurements of sample coated with Ni-P-ZnO



RMS(Roughness)	10 nm
Particle Size	47 nm
Grains	12

(b)

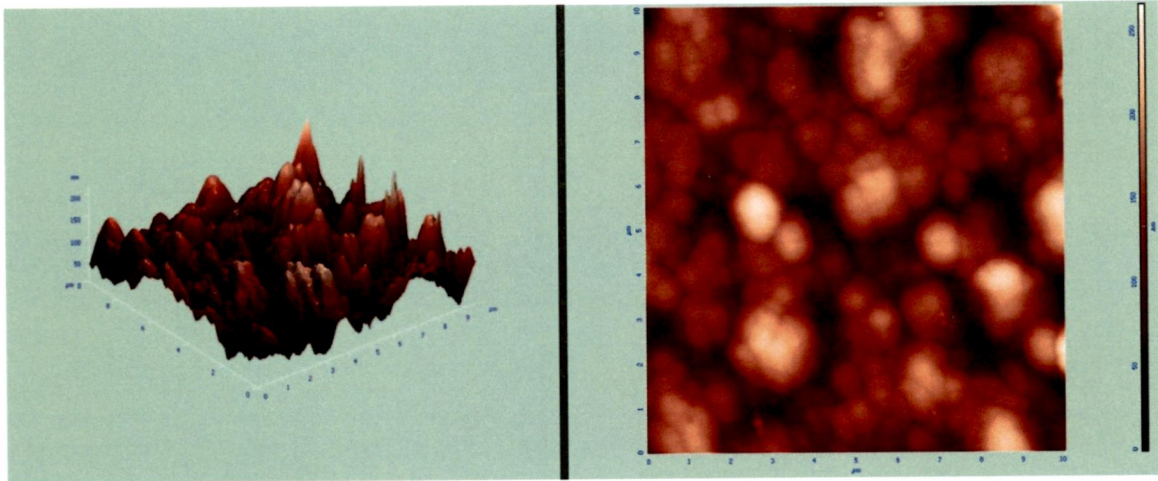
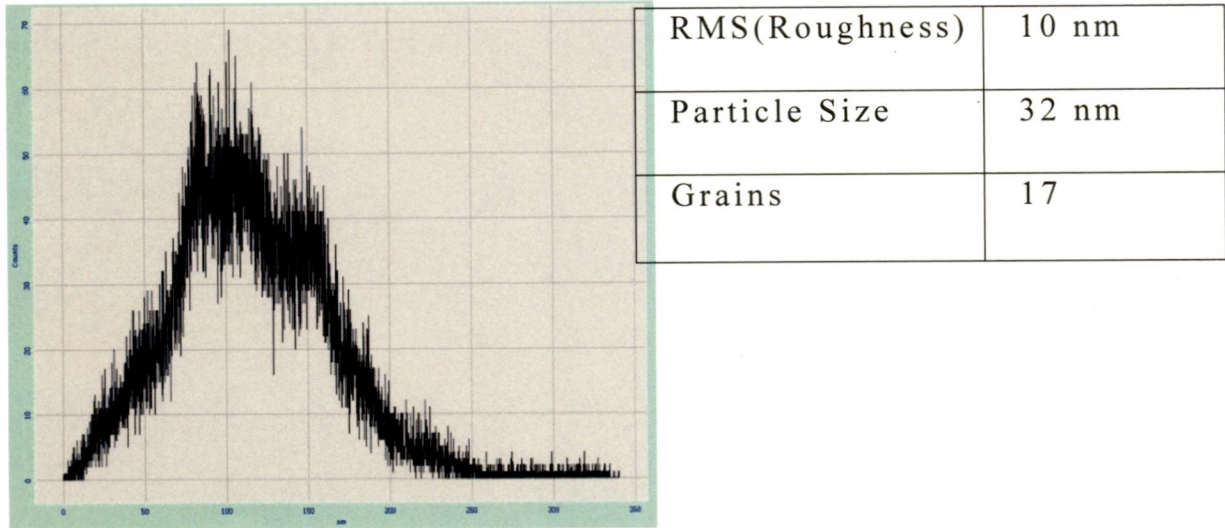


Table 5.3(c) AFM measurements of sample coated with Ni-P-ZnO after heat treatment



(c)

Fig:5.9 AFM Pattern showing 3D pattern, surface pattern, roughness of sample coated with (a) Ni-P; (b) Ni-P-ZnO and (c) Ni-P-ZnO after heat treatment

The roughness value shows the uniformity of surface coating more the roughness more is the abruptness the roughness value for the samples taken confirms the uniformity of the coating with little abruptness at certain points due to the third phase particles.

#### **5.2.5 Discussion:**

The X-Ray Diffraction results obtained for both the mechanochemical and sol-gel method confirm the presence of ZnO, the crystallite size obtained with mechanochemical method was 60 nm and the size obtained with sol-gel method was 20 nm. The X-Ray Diffraction studies and EDAX analysis of the coating obtained confirm the presence of ZnO particles in the coating. The particles when further coated with Ni-P aggregate in the bath since the average crystallite size of the ZnO peaks is 100 nm. The AFM studies show the uniformity of the coating.

## CONCLUSIONS

---

Following conclusions were made after performing and observing the experimental work reported in this thesis:

- Zinc oxide nanoparticles were successfully synthesized using mechano chemical synthesis
- The synthesized powders were characterized by X-Ray Diffraction studies by matching the peaks with the reported ones in JCPDS cards
- Amount of ZnO nanoparticles to be produced can be easily increased by increasing the initial quantity of the salts used.
- The average size obtained after 45 hours of milling was 60 nm.
- The average size after sol-gel method was 20 nm.
- The nano composite coating had successful incorporation of second phase particles as confirmed by X-Ray Diffraction and EDAX studies.
- The average size of ZnO coated in film was 100 nm this shows aggregation of nanoparticles in water.
- Deposition occurs on active sites only, the active sites develop on the substrate by first immersing the substrate into SnCl<sub>2</sub> solution and then in PdCl<sub>2</sub> solution.
- As the temperature of bath is increasing rate of reaction is also increasing so coating comes rapidly with increase in temperature. Since it is an autocatalytic reaction, which occurs faster at higher temperature.



## **FUTURE SCOPE**

---

Based on the results following work can be done in this field:

- Study of anti-microbial applications of the coating can be done since, ZnO nanoparticles are reported to have anti-microbial applications. The diffusion of the nanoparticles in the media is what is desired for this application. Hence, careful consideration is required.
- Effect of duration of coating process on spread of ZnO nanoparticles over the whole surface can be studied.
- Effect of different size nanoparticles on the applications of coating can be studied.
- Retention of the desired properties in coating that is a study of retentivity with time can be done to know the useful life of the coating.
- Incorporation of ZnO nanoparticles along with textile fabric can impart the properties to the cloth then produced. Hence, a study of incorporation in textile fabric can be carried out.
- Incorporation of Zinc oxide nanoparticles in medical sutures can be useful for imparting early healing, antimicrobial properties to the sutures.

## REFERENCES

---

- [1] Springer, Nanostructured thin films and nanodispersion strengthened coatings, edited by Andrey A. Voevodin, Dmitry V. Shtansky, Evgeny A. Levashov, John J. Moore pg. 91-92
- [2] MRS Bull. 2007, vol.32, Coyle, S., Wu, Y., Lau, K. T., De Rossi, D., and Wallace, G., pg. 434-442
- [3] Langmuir 2002 vol.18, Stoimenov, P. K., Klinger, R. L., Marchin, G. L., and Klabunde, K. J., Pg. 6679-6686
- [4] U.S. Patent 5,026,778, 2005, Organic, and Nano-Metal Chemistry (SRINMC), Taylor & Francis Group, LLC. Vol.36, 2006, Axtell, H. C., Hartley, S. M., and Sallavanti, R. A. pp. 493–515.
- [5] Z. Phys., 1953, E. Scharowski, 135-138.  
J. Mater. Sci., 1968, E. M. Dodson and J. A. Savage, 3-19
- [6] J. Cryst. Growth, 1972, R. Helbig, 15-25.
- [7] Chem. Phys. Lett. 407 (2005) X.Q. Meng, D.X. Zhao, J.Y. Zhang, D.Z. Shan, Y.M. Lu, Y.C. Liu, X.W. Fan, Growth temperature controlled shape variety of ZnO nanowires, 91–94.
- [8] J. Cryst. Growth 277 (2005) A. Umar, S. Lee, Y.S. Lee, K.S. Nahm, Y.B. Hahn, Star-shaped ZnO nanostructures on silicon by cyclic feeding chemical vapor deposition, 479–484.
- [9] Science 291 (2001) Z.W. Pan, Z.R. Dai, Z.L. Wang, Nanobelts of semiconducting oxides, 1947–1949.
- [10] Appl. Surf. Sci. 253 (2007) Rizwan Wahab, S.G. Ansari, Young-Soon Kim, Hyung-Kee Seo, Hyung-Shik Shin, Room temperature synthesis of needle-shaped ZnO nanorods via sonochemical Method, 7622–7626.
- [11] Mater. Res. Bull. 42 (2007) Rizwan Wahab, S.G. Ansari, Y.S. Kim, H.K. Seo, G.S. Kim, Gilson Khang, Hyung-Shik Shin, Low temperature solution synthesis and characterization of ZnO nano-flowers, 1640–1648.

- [12] Appl. Surf. Sci. 254 (2008) Rizwan Wahab, S.G. Ansari, Young Soon Kim, Gilson Khang, Hyung-Shik Shin, Effect of hydroxylamine hydrochloride on the floral decoration of zinc oxide synthesized by solution method, 2037–2042.
- [13] J. Phys. Chem. B 102 (1998) Eric A. Meulenkaamp, Synthesis and growth of ZnO nanoparticles, 5566–5572.
- [14] J. Am. Chem. Soc. 113 (1991) Lubomir Spanhel, Marc A. Anderson, Semiconductor clusters in the sol–gel process: quantized aggregation, gelation, and crystal growth in concentrated ZnO colloids, 2826–2833.
- [15] Chem. Mater. 14 (2002) Jun Zhang, Lingdong Sun, Jialu Yin, Huilan Su, Chun Sheng Liao, Chunhua Yan, Control of ZnO morphology via a simple solution route, 4172–4177.
- [16] Chem. Mater. 10 (1998) Ralph M. Nyffenegger, Ben Craft, Mohammed Shaaban, Sasha Gorer, George Erley, Rignald M. Penner, A hybrid electrochemical/chemical synthesis of zinc oxide nanoparticles and optically intrinsic thin films, 1120–1129.
- [17] C.J. Brinker, G.W. Scherer, Sol–Gel Science: The Physics and Chemistry of Sol–Gel Processing, Academic Press, San Deigo, 1990.
- [18] J. Metastable Nanocryst. Mater. 23 (2005) M.K. Hossain, S.C. Ghosh, Y. Bootongkang, C. Thanachayanont, J. Dutta, Growth of zinc oxide nanowires and nanobelts for gas sensing, 27–30.
- [19] J. Mater. Sci. 38 (2003) T. Hirano, H. Kozuka, Photonic properties of ZnO thin films prepared from zinc acetate solutions containing cobaltnacetate and polyvinylpyrrolidone, 4203–4210.
- [20] Appl. Phys. Lett. Vladimir A. Fonoberov, Alexander A. Balandina, Origin of ultraviolet photoluminescence in ZnO quantum dots: confined excitons versus surfacebound impurity exciton complexes, 85 (2004) 5971–5973.
- [21] J. Am. Ceram. Soc. 1964 R. A. Laudise, E. D. Kolb, A. J. Caporaso, , 47, 9.

- [22] M. Suscavage, M. Harris, D. Bliss, P. Yip, S. Q. Wang, D. Schwall, L. Bouthillette, J. Bailey, M. Callahan, D. C. Look, D. C. Reynolds, R. L. Jones, C. W. Litton, MRS Internet J. Nitride Semicond. Res. 1999, 4S1, G3.40.
- [23] Mater. Sci. Eng. B 2005, Y. H. Ni, X. W. Wei, H. M. Hong, Y. Ye, 121, 42.
- [24] Ceram. Int. 2000, C. H. Lu, C. H. Yeh, 26, 351.
- [25] Mater. Lett. 2005, Z. Hui, D. Yang, S. Z. Li, X. Y. Ma, Y. J. Ji, J. Xu, D. L. Que, 59, 1696.
- [26] Solid State Sci. 2005, H. W. Hou, Y. Xie, Q. Li, 7, 45.
- [27] Cryst. Res. Technol. 38 (2003), Wen Jun Li, Er Wei Shi, Tsuguo Fukuda, Particle size of powder under hydrothermal conditions, 847–858.
- [28] Nanotechnology 15 (2004), Hui Zhang, Deren Yang, Xiangyang Ma, Yujie Ji, Jin Xu, Duanlin Que, Synthesis of flower-like ZnO nanostructures by an organic-free hydrothermal process, 622–626.
- [29] Ceram. Int. 26 (2000), Chung Hsin Lu, Chi Hsien Yeh, Influence of hydrothermal conditions on the morphology and particle size of zinc oxide powder, 351–357.
- [30] Solar Energy Materials & Solar Cells 92 (2008), Seema Rani, Poonam Suri, P.K. Shishodia, R.M. Mehra, 1639–1645
- [31] Scripta Materialia. vol. 38, 1998, J. Apachitei, Duszczyk, L. Katgerman, and P.J.B. Overkamp, pp. 1383.
- [32] Z. Metallkunde. vol. 83, 1992, A. Srivastava, S. Mohan and V. Agarwala and R. C. Agarwala, pp. 251.
- [33] Nanotechnology 2005, C. Y. Lee, T. Y. Tseng, S. Y. Li, P. Lin, 16, 1105.
- [34] Nanotechnology 2005, vol.16, G. Q. Ding, M. J. Zheng, W. L. Xu, W. Z. Shen, 1285.
- [35] Journal of Physics: Conference Series 26 (2006), R Aghababazadeh, B Mazinani, A Mirhabibi And M Tamizifar 312–314
- [36] Scripta mater. 44 (2001), Tsuzuki T and McCormick P, 1731–1734.
- [37] Nanostruct. Mater., vol.8, 1997, Ding J, Tsuzuki T and McCormick P G, 75
- [38] Acta mater. 48 (2000), Tsuzuki T, McCormick P G, 2795-2801.
- [39] Metal-Organic, and Nano-Metal Chemistry (SRINMC), Taylor & Francis Group, LLC. 2006 vol.36, R.C. Agarwala, V. Agarwala and R. Sharma, pp. 493–515.
- [40] J. Res. Natl. Bur. Std. 1946, vol. 37, A. Brenner and E.J. Riddell, pp 31.
- [41] Brit. Pat. 1,041,753, U. S. Pat. vol. 3,644,183 and DDR Pat. 1966, vol. 41, Odekerken, pp. 406.

- [42] Woodhead Publishing limited. 1996, P. Gillespie, EL Nickel Coatings: Case Study, Surface Engineering Casebook, Ed. by Burnell J. S. Gray and P.K. Datta, pp. 49-54.
- [43] S.B. Sharma: PhD thesis Synthesis and Tribological characterization of Ni-P based Electroless composite coatings IIT Roorkee, India 2002.
- [44] Metal Finishing. 1983 vol. 81, N. Feldstein, T. Lancsek, D. Lindsay and L. Salerno, pp. 35.
- [45] Metal Finishing. 1984 vol. 82 ( 9), J. Henry, pp. 93.
- [46] R.C. Agarwala: PhD thesis Structural Studies and Crystallization behaviour of Electroless Ni-P Films IIT Roorkee (UOR), India 1987.
- [47] Meta. Mater. Trans. B., Vol. 36B, No.1, 2005, S. B. Sharma, R.C.Agarwala, V.Agarwala and K. G. Satyanarayana, pp. 23-31.
- [48] Z. Metallkunde 1992 vol. 83 (3), R.C. Agarwala and S. Ray: Crystallisation Behaviour of Electroless Ni-P Films: Part I, A Magnetic Moment study, pp. 199.
- [49] Z. Metallkunde. 1992 vol. 83 (3), R.C. Agarwala and S. Ray: Crystallisation Behaviour of Electroless Ni-P Films: Part II, A Magnetic Moment study, pp. 203.
- [50] Applied Surface Science. 2006 vol. 252, R. Sharma, R.C. Agarwala, V. Agarwala: Development of Copper Coatings on Ceramic Powder by Electroless Technique, pp. 8487.
- [51] Applied Surface Science. 2001, vol. 181, S. Sukla, S. Seal, J. Akasson, R. Order, R. Carter and Z. Rahaman, pp. 35.
- [52] Metal Finishing, 1985 vol. 83, J. Henry, pp. 372.
- [53] R.C. Agarwala and S. Ray: TEM investigation of the transformation during Annealing in Electroless Ni-P Films, Z. Metallkunde Bd., 1989 vol. 80, pp. 556.
- [54] Z. Metallkunde. 1992 vol. 83, A. Srivastava, S. Mohan and V. Agarwala and R. C. Agarwala, pp. 251.
- [55] Z. Metallkunde. 1992 vol. 83 (4), A. Srivastava, S. Mohan and V. Agarwala and R. C. Agarwala, pp. 254.
- [56] J. Am. Ceram. Soc. 1964, vol. 47, R. A. Laudise, E. D. Kolb, A. J. Caporaso, 9.
- [57] M. Suscavage, M. Harris, D. Bliss, P. Yip, S. Q. Wang, D. Schwall, L. Bouthillette, J. Bailey, M. Callahan, D. C. Look, D. C. Reynolds, R. L. Jones, C. W. Litton, MRS Internet J. Nitride Semicond. Res.1999, 4S1, G3.40.
- [58] Volume 252, Issue 24, 15 October 2006, Rahul Sharma, R.C. Agarwala and V. Agarwala Applied Surface Science, Pages 8487-8493
- [59] Journal of applied Electrochemistry, Vol. 33, Balaraju, J.N; Sankara Narayana, T. S. N; and Seshadri, S. K; (2003), " Electroless Ni-P Composite Coating", pp. 807-816.

- [60] H. E. Brown, *Zinc Oxide Rediscovered*, The New Jersey Zinc Company, New York (1957) and *Zinc Oxide, Properties and Applications* (1976).
- [61] *Appl. Surf. Sci.* 253 (2007), Rizwan Wahab, S.G. Ansari, Young-Soon Kim, Hyung-Kee Seo, Hyung-Shik Shin, Room temperature synthesis of needle-shaped ZnO nanorods via sonochemical Method, 7622–7626.
- [62] *Mater. Res. Bull.* 42 (2007), Rizwan Wahab, S.G. Ansari, Y.S. Kim, H.K. Seo, G.S. Kim, Gilson Khang, Hyung-Shik Shin, Low temperature solution synthesis and characterization of ZnO nano-flowers, 1640–1648.
- [63] *Appl. Surf. Sci.* 254 (2008), Rizwan Wahab, S.G. Ansari, Young Soon Kim, Gilson Khang, Hyung-Shik Shin, Effect of hydroxylamine hydrochloride on the floral decoration of zinc oxide synthesized by solution method, 2037–2042.
- [64] *J. Phys. Chem. B* 102 (1998), Eric A. Meulenkamp, Synthesis and growth of ZnO nanoparticles, 5566–5572.
- [65] *J. Am. Chem. Soc.* 113 (1991), Lubomir Spanhel, Marc A. Anderson, Semiconductor clusters in the sol–gel process: quantized aggregation, gelation, and crystal growth in concentrated ZnO colloids, 2826–2833.
- [66] *Chem. Mater.* 14 (2002), Jun Zhang, Lingdong Sun, Jialu Yin, Huilan Su, Chun Sheng Liao, Chunhua Yan, Control of ZnO morphology via a simple solution route, 4172–4177.
- [67] *Chem. Mater.* 10 (1998), Ralph M. Nyffenegger, Ben Craft, Mohammed Shaaban, Sasha Gorer, George Erley, Rignald M. Penner, A hybrid electrochemical/chemical synthesis of zinc oxide nanoparticles and optically intrinsic thin films, 1120–1129.